Master equation approach to the central spin decoherence problem: Uniform coupling model and role of projection operators

Edwin Barnes,[1,*] Łukasz Cywiński,[2,†] and S. Das Sarma[1]

[1]*Condensed Matter Theory Center, Department of Physics, University of Maryland, College Park, Maryland 20742-4111, USA*
[2]*Institute of Physics, Polish Academy of Sciences, Aleja Lotników 32/46, PL 02-668 Warszawa, Poland*

The generalized master equation of Nakajima-Zwanzig (NZ) type has been used extensively to investigate the coherence dynamics of the central spin model with a nuclear bath in a narrowed state characterized by a well-defined value of the Overhauser field. We reconsider the perturbative NZ approach and apply it to the exactly solvable case of a system with uniform hyperfine couplings. This is motivated by the fact that the effective-Hamiltonian-based theory suggests that the dynamics of the realistic system at low magnetic fields and short times can be mapped onto the uniform coupling model. We show that the standard NZ approach fails to reproduce the exact solution of this model beyond very short times, while the effective-Hamiltonian calculation agrees very well with the exact result on time scales during which most of the coherence is lost. Our key finding is that, in order to extend the time scale of applicability of the NZ approach in this case, instead of using a single projection operator one has to use a set of correlated projection operators which properly reflect the symmetries of the problem and greatly improve the convergence of the theory. This suggests that the correlated projection operators are crucial for a proper description of narrowed-state free-induction decay at short times and low magnetic fields. Our results thus provide important insights toward the development of a more complete theory of central spin decoherence applicable in a broader regime of time scales and magnetic fields.

I. INTRODUCTION

Qubits based on spins of single electrons confined in a semiconductor environment[1,2] are one of the most promising platforms for quantum computation. When the host semiconductor is a III–V compound material (i.e., GaAs or InAs), the presence of nuclear spins, coupled to the electron (or a hole) by hyperfine (hf) interaction, is unavoidable.[3,4] The qubit decoherence induced by hf interaction with such a nuclear bath has been a subject of many theoretical works. For this paper, the directly relevant ones are those focusing on purely hf-induced dynamics,[5–31] i.e., on the problem described by the central spin Hamiltonian

$$\hat{H} = \sum_k A_k \mathbf{S} \cdot \mathbf{I}_k + \Omega S^z + \sum_k \omega_k I_k^z, \qquad (1)$$

with $\mathbf{S}$ denoting the central spin, $\mathbf{I}_k$ the nuclear spins, A_k the hf couplings, and Ω and ω_k the central spin and nuclear spin Zeeman energies, respectively. This Hamiltonian can be solved exactly via Bethe ansatz[19,32,33] for the case of uniform $\omega_k = \omega$, where ω can be removed by going to a rotating frame.[9] However, it is very hard to extract potentially experimentally relevant information about the dynamics of the system, for example the time dependence of the reduced density matrix of the electron spin after initializing it in a pure state, when starting from the exact eigenstates,[19,30,34] and the largest system sizes considered had up to only $N = 30$ nuclear spins.[19] Numerical calculations of the system's evolution can also be obtained using the Chebyshev polynomial method,[8,35] which has been used to calculate the free-evolution[13] and spin-echo[27] signals for $N \leqslant 20$. Larger systems with $N \sim 10^4$ were investigated using an approximate spin-coherent-state P representation,[14,35] which, however, can only be used in the case of an unpolarized thermal nuclear bath, which is too restrictive for many applications including the

considerations presented here. In order to calculate the dynamics of the central spin on experimentally relevant time scales, and for experimentally relevant system sizes ($N \sim 10^4$–10^6 in III–V compound quantum dots), one has to resort to approximate analytical methods, which include the use of the generalized master equation (GME) of Nakajima-Zwanzig (NZ) type,[9,22,23,28] the GME of the time-convolutionless (TCL) kind,[22,24,36] and the cluster-expansion-type theories using the effective pure dephasing Hamiltonian,[4,12,25–27,36] obtained perturbatively from the original Hamiltonian of Eq. (1) by an appropriate canonical transformation.

In this paper we focus on the NZ theory applied to the case of *narrowed-state* free-induction decay (NFID), i.e., on the situation in which the nuclear system is prepared in an eigenstate of the Overhauser operator $h^z \equiv \sum_k A_k I_k^z$. This case is both important for quantum computation applications and experimentally relevant, since significant progress in nuclear-state narrowing has been made recently[37–41] (see also Ref. 3 and references therein). Furthermore, the high-magnetic-field regime of NFID (defined by the condition of $\Omega > \mathcal{A}$ where $\mathcal{A} \equiv \sum_k A_k \approx 90\ \mu\text{eV}$ in GaAs) was extensively investigated using the NZ approach.[9,23,28] Let us note that the other GME approaches, such as the TCL formalism and, more importantly in the context of this paper, the master equations employing correlated projection operators,[22,24,36] have been until now employed only in the case of thermal (non-narrowed) nuclear baths.

Let us briefly recount the main results of the NZ theory for the case of NFID. In the NZ approach, the equation of motion for the reduced density matrix of the central spin has an integro-differential form[42,43] with the memory kernel explicitly showing the influence of the history of the spin on its dynamics at a given point in time (i.e., the non-Markovian effects). While this feature is physically appealing

and offers a natural setting for investigation of the Markovian approximation and the corrections to it arising from the temporal nonlocality of the memory kernel, the NZ approach is technically very demanding. In the case of the central spin model, the memory kernel is expanded in powers of the flip-flop operator $V_{\rm ff} \sim S^{\pm} I^{\mp}$, and the expansion becomes very complicated with increasing order of perturbation theory. It also does not have any diagrammatic structure since it is not based on expanding a generalized (i.e., time- or contour-ordered) exponential, which would allow one to write down more easily higher-order contributions and identify the most important classes of terms at each order. Furthermore, the integro-differential equation is solved via Laplace transform, and the final result is obtained by inverse transform of a rather complicated expression.

Despite these obstacles, great progress has been made with this method. The second-order solution[9] was shown to reproduce the exact solution for the fully polarized bath case,[7] signifying the important role played by nuclear polarization (which limits the phase space for flip-flops) in improving the convergence of the NZ approach. For a general polarization, the second-order result was shown to lead to a very small coherence decay at high B fields satisfying $\mathcal{A}/\Omega \ll 1$. Specifically, the fraction of coherence lost was only about $\mathcal{A}^2/N\Omega^2 \ll 1$. A complete decay of the transverse electron spin components was obtained after going to the fourth order of the flip-flop expansion.[23,28] There, a controlled solution was obtained for $\mathcal{A}/\Omega < 1$ in the case of an unpolarized bath: after an initial quadratic decay shoulder, the decay was of the exponential form $\exp(-t/T_2)$, with $T_2 \sim N\Omega^2/\mathcal{A}^3$, with the $1/t^2$ tail appearing at very long times. Recently, it was shown[28] that with finite nuclear polarization, and for nuclear spin $I < 1$, it is possible to extend the fourth-order solution to lower B fields (down to $\mathcal{A}/\Omega \approx 1$ for unpolarized nuclei). As Ω is decreased, corrections to the above formula for T_2 appear, and at $\mathcal{A}/\Omega \approx 1$ a minimum of T_2 and a new kind of coherence envelope oscillation were predicted.[28]

It has to be stressed that most of the above features of the high-field NZ solution, especially the exponential decay, arise due to the inhomogeneous coupling of the nuclei to the central spin. In the fourth order in electron-nuclear flip-flops, the processes in which pairs of remote nuclei flip-flop with each other contribute to the system's dynamics. In the effective-Hamiltonian language,[12,16,23,25,26] one can say that the Overhauser field fluctuates due to electron-mediated flip-flops of these remote nuclei. At *short times* defined by $t \ll N/\mathcal{A} \sim 1/A_k$ the differences of Knight shifts $A_{kl} \equiv A_k - A_l$ of these nuclei are unimportant due to the energy-time uncertainty, leading to a quadratic decay shoulder that is independent of the wave function shape.[28] At longer times, the Knight shifts must fulfill more stringent energy conservation conditions, giving rise to long-time Markovian exponential decay, with the T_2 time strongly dependent on the shape of the wave function.[23] (Compare also the expressions for T_2 from Refs. 23 and 26 which correspond, respectively, to the two-dimensional Gaussian $e^{-(x^2+y^2)/a^2}$ and the same function modified by a cosine form factor in the z direction.)

An insight into the importance of the short-time regime is provided by theories based on an effective Hamiltonian, specifically Ring Diagram Theory (RDT), in which a class of diagrams of leading order in $1/N$ is resummed in the cluster expansion of the electron's density matrix.[4,25,26] According to these theories, for low fields such that $\mathcal{A}/\sqrt{N} \ll \Omega < \mathcal{A}$, most of the coherence decay occurs at short times, at which the distribution of the hf couplings does not matter and only the quantities $\mathcal{A}$ and N are important. This suggests that the low-field dynamics of NFID in a realistic system is closely related to dynamics in a system with *uniform* hf couplings.

In RDT, one starts with an approximate effective Hamiltonian derived in the second order of perturbation theory with respect to the flip-flop operator.[11,12,23,26] While this step makes it harder to precisely ascertain the limits of applicability of the approach, it allows for a very convenient formal simplification of the problem. The effective Hamiltonian is of the pure dephasing form, which allows for the use of standard tools of nonequilibrium quantum dynamics, such as the closed time-loop contour and the cluster expansion of the bath average of a generalized exponent.[17,25,26] Such methods were previously used in order to calculate decoherence for many other models of quantum baths;[44–46] however, in the spin bath case there are additional complications due to the lack of a simple Wick's theorem for spin operators. (See Refs. 17 and 47 for the derivation of all the diagrams in the fourth order of perturbation theory with respect to internuclear interactions.) However, for the electron-mediated (or hf-mediated) interactions, due to the fact that they couple all the N nuclear spins with comparable strength, one can resum all the leading diagrams in the $1/N$ expansion, which amounts to calculating only one diagram at each order of the cluster expansion.

For NFID at large B fields ($\mathcal{A}/\Omega \ll 1$), this resummation leads to an exponential decay with the same T_2 as the one obtained from the NZ approach[23,28] (albeit without the the $1/t^2$ long-time tail), down to $\mathcal{A}/\Omega \approx 1$, at which the minimum of T_2 is not reproduced. Within RDT one can calculate the short-time decoherence also at low magnetic fields obeying only the condition $\mathcal{A}/\sqrt{N}\Omega \ll 1$. The spin-echo signal predicted[25,26] by RDT was later seen in experiments on double GaAs quantum dots,[48] and it was recently rederived using an explicitly semiclassical approach.[31] For NFID, a decay envelope of the form $[1 + (t/\tau)^2]^{-1/2}$, with $\tau \sim N\Omega/\mathcal{A}^2$, and a $\pi/2$ phase shift of the electron precession for $t \gg \tau$ were predicted.[26] As we show explicitly in this paper, this result arises also as the large-N limit of the exact solution of the fully quantum calculation for the system with uniform hf couplings.

In this paper we apply the standard fourth-order NZ theory[9,23,28] to the otherwise exactly solvable model with uniform hf couplings. We find that the NZ calculation of NFID disagrees with the exact result beyond a very short time scale (at which the coherence barely decays), while the RDT calculation reproduces the envelope of the NFID signal very well. We show that, in order to improve the performance of the NZ theory, one needs to replace the commonly used single projection operator by a family of projection operators on nuclear subspaces which are singled out by the electron-nuclear coupling. Such an approach was used previously in both the NZ and TCL generalized master equation theories in the simpler case of a thermal nuclear bath,[22,24,36] but to our knowledge it has not been used until now for the *narrowed* FID case. This result strongly suggests that the main physics of the short-time and long-time

central spin decoherence is significantly different, with simple dephasing by distinct nuclear states dominating at short times, and nontrivial dynamics of inhomogeneously coupled nuclei dominating at long times. The use of the correlated projection operators allows the NZ theory to fully capture the short-time dynamics in a wide range of magnetic fields.

Let us briefly note that there exists a family of theories investigating the problem of dipolar-induced electron spin dephasing,[12,17,47,49–53] in which the dipolar-induced flip-flops between the nuclear spins lead to fluctuations of the Overhauser field. These theories, which are all based on some version of a linked cluster (cumulant expansion) theorem, are in agreement with the spin-echo measurements in phosphorus-doped silicon,[54] bismuth-doped silicon,[55] and GaAs singlet-triplet qubits at magnetic fields higher than $B \approx 0.3$ T.[48] The dipolar processes are indeed expected to dominate the decoherence at high B since the increasing qubit energy splitting is suppressing the dynamical processes due to hf interaction, while the dipolar flip-flops of the nuclei are practically unaffected by B. These experiments suggest that the window of parameters in which pure hf interactions dominate the electron spin decoherence is rather small in GaAs and Si. In fact, the spin-echo results in large GaAs dots[48] suggest that purely hf effects could be seen in lateral GaAs dots only at $B < 0.3$ T. However, it was suggested that in small and strained InGaAs quantum dots the dipolar interactions between the nuclei might be suppressed by strongly inhomogeneous Knight shifts and by the quadrupolar interactions.[28] Experimental results suggesting suppression of dipolar-induced spin diffusion in such dots have appeared recently.[56]

Notwithstanding the future experimental developments, which hopefully will allow for measurements of purely hf-induced decoherence in a wide range of B fields, spanning the short-time semiclassical and long-time Markovian regimes (with possible nontrivial crossover between them suggested by the results of Ref. 28), the central spin decoherence problem remains theoretically interesting in itself. We hope that its further investigation will lead to establishing deeper connections between various approaches known from the theory of open quantum systems, and the properties of the exact Bethe ansatz solution.

The paper is organized in the following way. In Sec. II, we introduce the hyperfine Hamiltonian and give the explicit form of the initial nuclear density matrix characterizing NFID. In Sec. III, we present the exact solution of NFID for the uniform coupling model. Section IV offers an extensive review of the Nakajima-Zwanzig master equation treatment of the central spin model, with the electron spin coherence computed up to fourth order in the hyperfine flip-flop interaction. This section, together with the detailed Appendixes A and B, can be mostly skipped by a reader deeply familiar with previous derivations of this theory.[9,28] However, we hope that our derivations, apart from making the paper self-contained, are useful additions to the existing works, clarifying some technical issues and expanding the discussion of certain aspects of a highly technical theory. In the subsequent Sec. V, we present a derivation of NFID in the uniform coupling model using the fourth-order NZ approach and show that the results disagree with the exact solution except at very early times.

We demonstrate that the strong discrepancy between the exact and NZ solutions can be lifted by replacing the standard single projection operator in the NZ theory with a family of correlated projection (CP) operators, and that the modified NZ theory (which we refer to as the NZ-CP theory) then gives results which are indistinguishable from the exact solution. We further show that the NZ-CP result is closely related to and improves upon that which is obtained by applying RDT to the uniform coupling model. The reasons for this behavior of the NZ theory, together with the implications of these findings for coherence decay in realistic systems with nonuniform couplings, are discussed in Sec. VI.

II. HAMILTONIAN AND INITIAL NUCLEAR BATH STATE

The Hamiltonian for a single electron spin coupled to a nuclear spin bath via the hyperfine interaction has the form

$$H = H_0 + V_{\text{ff}}, \tag{2}$$

$$H_0 = \Omega S^z + \sum_k \omega_k I_k^z + S^z h^z, \tag{3}$$

$$V_{\text{ff}} = \tfrac{1}{2}(h^+ S^- + h^- S^+), \tag{4}$$

with

$$h^i \equiv \sum_k A_k I_k^i. \tag{5}$$

The S^i are the components of the electron spin operator, while the I_k^i are the components of the spin operator for the kth nucleus. The electron spin raising and lowering operators $S^\pm$ and their nuclear counterparts are defined in the usual way:

$$S^\pm = S^x \pm i S^y, \quad I_k^\pm = I_k^x \pm i I_k^y. \tag{6}$$

We have included a magnetic field which points in the z direction, and Ω and ω_k are the Zeeman energies of the electron and nuclei. In order to properly describe the nuclear bath in III–V semiconductors, we should allow for several different isotopic species of nuclei. Rather than introduce an extra index to label distinct nuclear species, we have absorbed this index into the site index k on the hyperfine couplings A_k and nuclear Zeeman energies ω_k. These quantities will in general depend on the nuclear species since different species will have different gyromagnetic factors. For example, the hyperfine couplings are given by $A_k = \nu_0 \mathcal{A}_\alpha |\Psi(r_k)|^2$, where ν_0 is the volume of the primitive unit cell, $\Psi(r_k)$ is the electron envelope wave function evaluated at the position r_k of the kth nucleus, and $\mathcal{A}_\alpha$ is the total hyperfine interaction energy between the electron and a nucleus of species α and depends on the electron and nuclear spin gyromagnetic factors.

The sums in Eqs. (2)–(5) range over some number N of nuclei which comprise the bath. Quantum dots residing in III–V materials like GaAs and InAs typically contain 10^4–10^6 nuclei which interact appreciably with the electron, so physical values of N should lie in this range, although in analytical calculations often one simply performs a sum over an infinite number of spins (out of which only about N are appreciably coupled to the electron spin). It is often useful to define the

"effective number of nuclei appreciably interacting with the electron" N:

$$N \equiv \frac{\mathcal{A}^2}{\sum_k A_k^2}, \tag{7}$$

where

$$\mathcal{A} \equiv \sum_k A_k \tag{8}$$

is the total hyperfine interaction energy between the electron and the nuclear bath. For the most part, we will leave N arbitrary in subsequent sections, but when a more precise definition is necessary, we will use Eq. (7).

Let us quote some numbers in order to make a connection to experimentally relevant time scales and magnetic field regimes. In GaAs, $\mathcal{A} \approx 90 \, \mu\text{eV}$ (see, e.g., Ref. 3 and references therein). Using the effective g factor $g_{\text{eff}} \approx 0.5$ of an electron in this material, $\Omega \approx \mathcal{A}$ for a magnetic field of $B \approx 3$ T. Another characteristic magnetic field in the central spin problem is that corresponding to the typical Overhauser field for a thermal nuclear bath, $\mathcal{A}/\sqrt{N}$, which is on the order of a few millitesla. Note that the maximal hf coupling of a nuclear spin is $A_k \sim \mathcal{A}/N$, which is much smaller than Ω for the magnetic fields considered in this paper (i.e., fields such that $\Omega > \mathcal{A}/\sqrt{N}$). An important quantity is also the time scale of $N/\mathcal{A}$, defining here the boundary of the short-time regime. For $N = 10^4$–10^6 this corresponds to time scales of 100 ns–10 μs.

It is difficult to obtain explicit results from the NZ GME unless strong assumptions are made about the form of the initial nuclear density matrix, which we denote $\rho_I(0)$. Fortunately, the NZ GME seems most tractable in the case of NFID, which is the primary focus of the present work. As we develop the structure of the NZ GME adapted to the central spin problem in Sec. IV, we will attempt to keep the form of $\rho_I(0)$ as general as possible at each stage of the calculation and make clear the points at which it is necessary to further specify $\rho_I(0)$. For the sake of clarity, we will state here the precise final form that we will impose on $\rho_I(0)$ in order to obtain explicit results for the electron spin coherence in the NFID case.

In discussing the initial density matrix of the nuclei, we have already alluded to the first assumption we will make about the initial conditions, namely, that the initial density matrix for the total system is separable:

$$\rho(0) = \rho_e(0) \otimes \rho_I(0). \tag{9}$$

Here, ρ_e is the reduced density matrix describing the electron spin degrees of freedom. This assumption is quite reasonable since, in quantum computing applications, it is generally desirable to initialize the electron spin to some well-defined state which is independent of the nuclei.

In contrast, a much stronger assumption we will make is that $\rho_I(0)$ is diagonal in the basis of h^z eigenstates. As in Refs. 9 and 28, we will denote these states by $|n_i\rangle$ with $i = 1, \ldots, 2^N$; they are just tensor products of eigenstates of the nuclear spin operators I_k^z:

$$|n_i\rangle = \bigotimes_k |I_k, m_k^i\rangle, \quad I_k^z |I_k, m_k^i\rangle = m_k^i |I_k, m_k^i\rangle, \tag{10}$$

where I_k is the spin of the kth nucleus. We may write

$$h^z |n_i\rangle = h_{n_i}^z |n_i\rangle, \quad h_{n_i}^z \equiv \sum_k A_k m_k^i. \tag{11}$$

We will further assume that $\rho_I(0)$ only contains components which share the same h^z eigenvalue, denoted h_n^z:

$$\rho_I(0) = \sum_{i=1}^{g} \rho_{ii} |n_i\rangle\langle n_i|, \tag{12}$$

where

$$h^z |n_i\rangle = h_n^z |n_i\rangle, \quad \forall \; i \in 1, \ldots, g, \tag{13}$$

The form of the density matrix given in (12) and (13) describes a particular "narrowed" set of allowed states for the nuclear bath.[9] In the so-called box model limit where the hyperfine couplings are all equal, $A_k = A = \mathcal{A}/N$, this amounts to restricting the possible nuclear states to a set which contains only states with a fixed net polarization along the magnetic field direction. We will see that the NZ GME approach enjoys many simplifications when the nuclear bath states are constrained in this way.

For some of the more explicit results we will obtain, we will also follow Refs. 9 and 28 in assuming that the nuclear spin bath is uniformly polarized. By this, we mean that all traces of nuclear spin operators are independent of the nuclear site indices. For example, the correlator

$$\text{Tr}\{I_p^+ I_q^- \rho_I(0) I_k^- I_\ell^+\} \tag{14}$$

is independent of k, ℓ, p, q under this supposition. The uniform polarization assumption is less crucial than the narrowed-state condition of Eq. (12) and can be lifted in most cases, albeit at the expense of having to deal with more complicated algebraic expressions. For the purposes of elucidating more general features of the NZ GME approach, it is often a useful assumption to make. Throughout this paper we make explicit the points at which we invoke the uniform polarization condition.

III. UNIFORM COUPLING MODEL

In this section, we will consider the uniform coupling (also referred to as the box model) limit in which all the hyperfine couplings are equal,

$$A_k = A \equiv \frac{\mathcal{A}}{N}. \tag{15}$$

This is a semiclassical limit of the central spin problem since we have a large collective nuclear spin $\mathbf{I} = \sum_k \mathbf{I}_k$ coupled to the electron spin—the dynamics is mostly classical for large N. This is also very close to the static bath limit: for $\Omega \gg \mathcal{A}/\sqrt{N}$ and for a typical collective spin magnitude $|I| \approx \sqrt{N}$, $\mathbf{I}$ is almost static as it cannot follow the quickly precessing electron spin vector (if we neglect the nuclear Larmor precession, which is crucial for the case of spin-echo decay,[25,26,31,48] but which is of much smaller importance for NFID).

The limit of uniform hyperfine couplings greatly simplifies the electron-nuclear dynamics, making this a natural limit in which to compare various approaches to the problem. In particular, this limit is exactly solvable,[7,13,20,22,27,57] and we

will begin by reviewing this solution for the NFID case. In Sec. V, we will use this solution to test how well the NZ approach (both the standard one and the one using correlated projection operators) can describe the dynamics of the box model.

Restricting attention to the homonuclear case $\omega_k = \omega$, with all the nuclei having spin $I = 1/2$, we can solve the uniform coupling model exactly by working in the basis of eigenstates of the total nuclear spin operator $I^z = \sum_k I_k^z$; we denote these states by $|jm\rangle$ with $I^z|jm\rangle = m|jm\rangle$. In this basis, we may write the expectation value $\langle S^+(t)\rangle$ in terms of the appropriate matrix element of the reduced density matrix evolved with respect to the full Hamiltonian:

$$\langle S^+(t)\rangle = \sum_{jm} n_j \langle \downarrow, j, m | e^{-iHt} \rho(0) e^{iHt} | \uparrow, j, m \rangle. \quad (16)$$

The $\uparrow$, $\downarrow$ inside the kets denote the eigenstates of the electron spin operator S^z. $\rho(0)$ is the full density matrix at time $t = 0$, and n_j is the degeneracy of nuclear states with a fixed j and m,[58]

$$n_j = \frac{N!}{\left(\frac{N}{2} - j\right)!\left(\frac{N}{2} + j\right)!} \frac{2j + 1}{\frac{N}{2} + j + 1}. \quad (17)$$

In order to facilitate the computation, we will assume that the initial nuclear density matrix is diagonal in the $|jm\rangle$ basis. In fact, in order to compare with the NZ GME result computed in Sec. V, we will assume that the initial nuclear density matrix is proportional to the identity in a subspace of fixed m and is zero outside this subspace. This is equivalent to the form of $\rho_I(0)$ that we assumed in Eqs. (12) and (13), if in the latter we make the further assumption that the nuclei are uniformly polarized, $\rho_{ii} = 1/Z$ with $Z = \sum_j n_j$. When the density matrix has this form, our formula becomes

$$\langle S^+(t)\rangle = \frac{1}{Z} \sum_{j=|m|}^{N/2} n_j \langle \downarrow, j, m | e^{-iHt} \rho_e(0) e^{iHt} | \uparrow, j, m \rangle, \quad (18)$$

where $\rho_e(0)$ is the initial electron density matrix.

In the case where all hyperfine couplings are equal, $A_k = A$, it is straightforward to work out the action of the evolution operator e^{-iHt} on the $|\uparrow/\downarrow, j, m\rangle$ states:[22,27]

$$e^{-iHt} | \uparrow, j, m \rangle = a_{jm} | \uparrow, j, m \rangle + b_{jm} | \downarrow, j, m + 1 \rangle,$$
$$e^{-iHt} | \downarrow, j, m \rangle = c_{jm} | \downarrow, j, m \rangle + d_{jm} | \uparrow, j, m - 1 \rangle, \quad (19)$$

with

$$a_{jm} = e^{-iE_m^+ t}\left[\cos\left(\frac{N_{jm}^+}{2}t\right) - i\frac{Z_m^+}{N_{jm}^+}\sin\left(\frac{N_{jm}^+}{2}t\right)\right],$$

$$b_{jm} = -i e^{-iE_m^+ t}\frac{X_{jm}^+}{N_{jm}^+}\sin\left(\frac{N_{jm}^+}{2}t\right),$$

$$\quad (20)$$

$$c_{jm} = e^{-iE_m^- t}\left[\cos\left(\frac{N_{jm}^-}{2}t\right) - i\frac{Z_m^-}{N_{jm}^-}\sin\left(\frac{N_{jm}^-}{2}t\right)\right],$$

$$d_{jm} = -i e^{-iE_m^- t}\frac{X_{jm}^-}{N_{jm}^-}\sin\left(\frac{N_{jm}^-}{2}t\right),$$

and

$$E_m^\pm = (m \pm 1/2)\omega - \mathcal{A}/(4N),$$
$$X_{jm}^\pm = \mathcal{A}\sqrt{j(j+1) - m(m\pm 1)}/N,$$
$$Z_m^\pm = \pm[\Omega - \omega + \mathcal{A}(m \pm 1/2)/N],$$
$$N_{jm}^\pm = \sqrt{(X_{jm}^\pm)^2 + (Z_m^\pm)^2}. \quad (21)$$

Using (19) and expanding the initial electron density matrix as

$$\rho_e(0) = \tfrac{1}{2}\mathbf{1} + 2\langle S^z(0)\rangle S^z + \langle S^+(0)\rangle S^- + \langle S^-(0)\rangle S^+, \quad (22)$$

one finds that only the S^- component of $\rho_e(0)$ contributes to $\langle S^+(t)\rangle$:

$$\langle S^+\rangle = \frac{\langle S^+(0)\rangle}{Z} \sum_{j=|m|}^{N/2} n_j \langle \downarrow, j, m | e^{-iHt} S^- e^{iHt} | \uparrow, j, m \rangle$$

$$= \frac{\langle S^+(0)\rangle}{Z} \sum_{j=|m|}^{N/2} n_j a_{jm}^* c_{jm}. \quad (23)$$

For later comparison, we transform this result to a certain rotating frame defined with respect to the frequency $\Omega_n + \Delta\Omega$, where

$$\Omega_n \equiv \Omega + h_n^z, \quad (24)$$

and the "Lamb shift" $\Delta\Omega$ will be defined later on. In the rotating frame, the exact solution to the uniform coupling model is then given by

$$x_{\text{exact}}(t) = \frac{x_0}{Z} e^{-i(\Omega + \mathcal{A}m/N + \Delta\Omega)t} \sum_{j=|m|}^{N/2} n_j a_{jm}^* c_{jm}. \quad (25)$$

To obtain this expression, we have used that $h_n^z = \mathcal{A}m/N$ in the case of uniform coupling.

IV. NAKAJIMA-ZWANZIG MASTER EQUATION AND ITS PERTURBATIVE EXPANSION

The first step in constructing the NZ GME is to separate the density matrix for the total system into two parts, often referred to as the relevant and the irrelevant parts:[42,43]

$$\rho = \rho_{\text{rel}} + \rho_{\text{irr}}. \quad (26)$$

The relevant part ρ_{rel} is a density matrix for the degrees of freedom whose evolution one wishes to compute, while the irrelevant part ρ_{irr} contains the remaining degrees of freedom in the total system. While these remaining degrees of freedom will influence the evolution of ρ_{rel}, their own evolution is not of direct concern and need not be computed explicitly. In applications where one considers the dynamics of a system coupled to a bath, ρ_{rel} is typically a density matrix describing the degrees of freedom of the system. In this case, note that, strictly speaking, ρ_{irr} is not a density matrix since it does not satisfy $\text{Tr}\rho_{\text{irr}} = 1$.

The partition described in Eq. (26) is implemented by introducing projection superoperators P and Q such that

$$P\rho = \rho_{\text{rel}}, \quad Q\rho = \rho_{\text{irr}}, \quad P + Q = 1, \quad PQ = 0. \quad (27)$$

The last two relations above ensure that P and Q are true projectors in the sense that $P^2 = P$ and $Q^2 = Q$. With these

operators, the Liouville equation for ρ can be transformed into an exact equation for the evolution of ρ_{rel}, which in the case of a time-independent Hamiltonian H has the form[42,43]

$$P\dot{\rho}(t) = -iPLP\rho(t) - i\int_0^t dt'\,\widehat{\Sigma}(t-t')P\rho(t'), \quad (28)$$

$$\widehat{\Sigma}(t) \equiv -iPLQe^{-iLQt}QLP. \quad (29)$$

The Liouvillian superoperator L implements the evolution of the total system and is defined to act on an arbitrary operator $\mathcal{O}$ according to

$$L\mathcal{O} = [H,\mathcal{O}]. \quad (30)$$

The superoperator $\widehat{\Sigma}$ is referred to as the memory kernel; this quantity contains the full dynamics of the bath and controls how this dynamics affects the evolution of the system. It is important to note that the particular form of the NZ equation given in Eq. (28) assumes that the initial density matrix satisfies the condition $Q\rho(0) = 0$.

In the case of our central spin model, Eqs. (2)–(5), we choose ρ_{rel} to be essentially the reduced density matrix for the electron spin ρ_e. This means that the projection operator P involves a trace over the nuclear bath:[9,23,28]

$$P\rho = \rho_I(0)\text{Tr}_I\rho = \rho_e \otimes \rho_I(0). \quad (31)$$

We have introduced a factor of the initial nuclear density matrix $\rho_I(0)$ in the definition of P to satisfy the constraint $P^2 = P$. Note that the condition $Q\rho(0) = 0$ is tantamount to assuming that $\rho(0)$ is separable:

$$\rho(0) = \rho_e(0) \otimes \rho_I(0). \quad (32)$$

This is an assumption we will make throughout this work.

It is important to stress that Eq. (31) is not the only possible choice for the projector P. For example, it is possible to instead define P as a sum over many projection operators which project onto various subspaces of the nuclear bath state space, and the choice of P can strongly influence the convergence properties of the resulting theory.[22,24] In fact, we will see later on in the context of the uniform coupling model that the choice made in Eq. (31) is far from ideal, and that a more sophisticated choice leads to a vast improvement in the convergence of the theory. Given the connection between the box model and the short-time, low-B-field regime of the real system with nonuniform couplings, we will argue that this observation carries important consequences for the development of a more complete theory of the central spin problem. For now, we will keep the definition of P in Eq. (31) and continue our construction of the "standard" NZ theory.

The form of the NZ equation given in Eq. (28) is quite difficult to work with. In order to reduce it to a more tractable form, we will place restrictions on the structure of the initial nuclear density matrix $\rho_I(0)$. In particular, we will assume that $\rho_I(0)$ is diagonal in the $|n_i\rangle$ basis: $\rho_I(0) = \sum_i \rho_{ii}|n_i\rangle\langle n_i|$. If we then multiply both sides of Eq. (28) by the operator S^+ and take the trace, we obtain an equation for $\langle S^+\rangle$ only:

$$\frac{d}{dt}\langle S^+(t)\rangle = i\Omega_n\langle S^+(t)\rangle - i\int_0^t dt'\Sigma(t-t')\langle S^+(t')\rangle, \quad (33)$$

where $\Omega_n \equiv \Omega + h_n^z$ with

$$h_n^z \equiv \text{Tr}_I[h^z\rho_I(0)] = \sum_i \rho_{ii}h_{n_i}^z. \quad (34)$$

Note that this definition of h_n^z is more general than the meaning we gave this symbol in Eq. (13) in the context of the fully restricted nuclear density matrix. The two meanings coincide when $\rho_I(0)$ has the form of Eq. (12). The memory kernel is now a function instead of an operator:

$$\Sigma(t) \equiv -i\text{Tr}[S^+PLQe^{-iLQt}QLPS^-\rho_I(0)]. \quad (35)$$

Without the assumption that $\rho_I(0)$ is diagonal in the $|n_i\rangle$ basis, additional terms involving $\langle S^z(t)\rangle$ and $\langle S^-(t)\rangle$ appear in Eq. (33), and the problem becomes considerably more complicated. Note that we did not have to assume the fully restricted form for $\rho_I(0)$ quoted in Eq. (12) where the sum is only over $|n_i\rangle$ states corresponding to the same Overhauser field. Equation (33) is valid when the sum contains other states as well, i.e., when the nuclear state is not narrowed.

Equation (33) is an integro-differential equation which can easily be solved by performing a Laplace transform, after which the equation becomes algebraic with the solution

$$\langle S^+(s)\rangle = \int_0^\infty dt\, e^{-st}\langle S^+(t)\rangle = \frac{\langle S^+(t=0)\rangle}{s - i\Omega_n + i\Sigma(s)}. \quad (36)$$

The solution in the time domain is then obtained by computing the Bromwich inversion integral,

$$\langle S^+(t)\rangle = \frac{1}{2\pi i}\int_{\gamma-i\infty}^{\gamma+i\infty} ds\, e^{st}\langle S^+(s)\rangle, \quad (37)$$

where the contour defined by the real number γ must be chosen such that it lies to the right of all the poles of $\langle S^+(s)\rangle$. Therefore, solving for $\langle S^+(t)\rangle$ requires solving for the Laplace transform of the memory kernel:

$$\begin{aligned}\Sigma(s) &= \int_0^\infty dt\, e^{-st}\Sigma(t) \\ &= -i\text{Tr}\left[S^+PLQ\frac{1}{s+iLQ}QLPS^-\rho_I(0)\right]. \end{aligned} \quad (38)$$

Exact computation of the memory kernel is a difficult problem except in very simple cases, so we will proceed to calculate it perturbatively in the following section.

A. The expansion of the memory kernel

In order to make further progress, it is necessary to construct a perturbative expansion of the memory kernel given in Eq. (38). We will expand this quantity in a power series in the number of flip-flops, i.e., in powers of V_{ff}:

$$\Sigma(s) = \Sigma^{(2)}(s) + \Sigma^{(4)}(s) + O(V_{\text{ff}}^6). \quad (39)$$

We can have only even terms in this expansion since the flip-flops are virtual in the physical limit $\Omega \gg \omega_k$. For nuclear density matrices $\rho_I(0)$ which are diagonal in the $|n_i\rangle$ basis, the odd terms are strictly zero due to the structure of the memory kernel, Eq. (38). We will see shortly why a zeroth-order term has not been included in Eq. (39).

To facilitate the expansion, it is convenient to define the following superoperators:

$$L_0\mathcal{O} = [H_0,\mathcal{O}], \quad (40)$$

$$L_V\mathcal{O} = [V_{\text{ff}},\mathcal{O}]. \quad (41)$$

Replacing $L \to L_0 + L_V$ in (38), we can then recast our perturbative flip-flop expansion as an expansion in L_V. The expansion of the memory kernel is tantamount to an expansion of the operator $\frac{1}{s+i(L_0+L_V)Q}$ in powers of L_V, and this series is straightforward to construct:

$$\frac{1}{s+iLQ}$$
$$= \{1 - iG_Q(s)L_VQ - G_Q(s)L_VQG_Q(s)L_VQ$$
$$+ iG_Q(s)L_VQG_Q(s)L_VQG_Q(s)L_VQ\}G_Q(s) + O\left(L_V^4\right),$$
$$\tag{42}$$

where

$$G_Q(s) \equiv \frac{1}{s+iL_0Q}. \tag{43}$$

Using this expansion, we will compute the memory kernel up to fourth order.

Before we proceed to compute the terms of the series, we first pause to write down some identities which will be useful at various stages of the expansion. When $\rho_I(0)$ is diagonal in the $|n_i\rangle$ basis, the following identity holds for any integers k and ℓ:

$$PL_0^k L_V L_0^\ell P = 0. \tag{44}$$

This identity can be further generalized to include any combination of L_0's and an odd number of L_V's sandwiched between two P's. When $\rho_I(0)$ is further restricted to the form given in Eq. (12), we have an additional identity (expressed in two equivalent ways):

$$QL_0P = 0, \quad QL_0Q = QL_0. \tag{45}$$

The first form of this identity allows us to replace one of the L's in Eq. (38) with L_V:

$$\Sigma(t) = -i\text{Tr}\left[S^+PLQ\frac{1}{s+iLQ}QL_VPS^-\rho_I(0)\right], \tag{46}$$

which indicates that the zeroth-order memory kernel vanishes, as was already presumed in (39). Note that in using Eq. (45) to arrive at Eq. (46), we are assuming the fully restricted form of $\rho_I(0)$ stated in Eqs. (12) and (13), whereas up until now we have needed to assume only that $\rho_I(0)$ is diagonal in the $|n_i\rangle$ basis. In fact, at this point it is not really necessary to impose Eq. (12), and we could instead continue to suppose only that $\rho_I(0)$ is diagonal, in which case we would find a nonvanishing zeroth-order term in the memory kernel expansion. However, slightly further into the calculation we will impose Eqs. (12) and (13), and so at this stage we may as well make the simplifications that this form of $\rho_I(0)$ brings.

B. Second-order memory kernel

Inserting Eq. (42) into Eq. (46), we find at second order

$$\Sigma^{(2)}(s) = -i\text{Tr}[S^+PL_VQG_Q(s)QL_VPS^-\rho_I(0)]$$
$$- \text{Tr}[S^+PL_0QG_Q(s)L_VQG_Q(s)QL_VPS^-\rho_I(0)]. \tag{47}$$

The second term on the right-hand side can be shown to vanish identically for the central spin Hamiltonian. Focusing then on

the first term, this expression is somewhat complicated by the dependence of $G_Q(s)$ on Q. Instead of working with $G_Q(s)$, we choose to work with its time-domain counterpart e^{-iL_0Qt}, in terms of which we have

$$\Sigma^{(2)}(t) = -i\text{Tr}[S^+PL_VQe^{-iL_0Qt}QL_VPS^-\rho_I(0)]. \tag{48}$$

It is easy to show that the identity (45) enables the extraction of the projection operator Q from the exponent:

$$Qe^{-iL_0Qt} = Qe^{-iL_0t} \equiv QG(t). \tag{49}$$

The superoperator $G(t)$ is simply the evolution operator corresponding to the unperturbed part of the Hamiltonian H_0:

$$G(t)\rho(0) = e^{-iH_0t}\rho(0)e^{iH_0t}. \tag{50}$$

Also notice that (49) immediately implies

$$QG_Q(s) = QG(s), \tag{51}$$

with the "propagator" defined as

$$G(s) \equiv \frac{1}{s+iL_0}. \tag{52}$$

At this point, we will invoke [by using Eq. (45)] the most constrained form of the initial nuclear density matrix, Eqs. (12) and (13), as it is not clear how to proceed without factoring the projector Q out of the propagator $G(s)$. If one could proceed without performing this factorization, then it would suffice to assume only that $\rho_I(0)$ is diagonal in the $|n_i\rangle$ basis, albeit several more terms would contribute at each order of the memory kernel expansion. In any case, we are ultimately interested in applying this formalism to the case of NFID, which is defined precisely by Eqs. (12) and (13).

Plugging Eq. (49) into Eq. (48), eliminating factors of Q with applications of the identity given in Eq. (44), and dropping factors of P using the observations that $PS^-\rho_I(0) = S^-\rho_I(0)$ and $\text{Tr}[S^+P\mathcal{O}] = \text{Tr}[S^+\mathcal{O}]$ for any operator $\mathcal{O}$, we arrive at

$$\Sigma^{(2)}(t) = -i\text{Tr}[S^+L_VG(t)L_VS^-\rho_I(0)]. \tag{53}$$

It remains to plug in explicit expressions for the various operators and perform the trace. Defining the following set of operators which act in the nuclear subspace:

$$U_\pm(t) \equiv e^{\mp(i/2)(\Omega+h^z)t-i\sum_k \omega_k I_k^z t}, \tag{54}$$

we can express the action of $G(t)$ on a matrix ρ as

$$G\rho = \begin{pmatrix} U_+\rho_{\uparrow\uparrow}U_+^\dagger & U_+\rho_{\uparrow\downarrow}U_-^\dagger \\ U_-\rho_{\downarrow\uparrow}U_+^\dagger & U_-\rho_{\downarrow\downarrow}U_-^\dagger \end{pmatrix}, \tag{55}$$

while the action of L_V has the explicit form

$$L_V\rho = \frac{1}{2}\begin{pmatrix} h^-\rho_{\downarrow\uparrow} - \rho_{\uparrow\downarrow}h^+ & h^-\rho_{\downarrow\downarrow} - \rho_{\uparrow\uparrow}h^- \\ h^+\rho_{\uparrow\uparrow} - \rho_{\downarrow\downarrow}h^+ & h^+\rho_{\uparrow\downarrow} - \rho_{\downarrow\uparrow}h^- \end{pmatrix}, \tag{56}$$

where, for instance, $\rho_{\uparrow\downarrow} = \langle\uparrow|\rho|\downarrow\rangle$, with $|\uparrow\rangle$ and $|\downarrow\rangle$ denoting the eigenstates of the electron spin operator S^z. After a bit of algebra, we find

$$\Sigma^{(2)}(t) = \frac{1}{4i}\sum_k A_k^2 e^{i\omega_k t}[c_k^- e^{i(A_k/2)t} + c_k^+ e^{-i(A_k/2)t}], \tag{57}$$

where

$$c_k^\pm \equiv \mathrm{Tr}\{I_k^\mp I_k^\pm \rho_I(0)\}. \tag{58}$$

The Laplace transform of this is

$$\Sigma^{(2)}(s) = \frac{1}{4i} \sum_k A_k^2 \left[\frac{c_k^+}{s - i\left(\omega_k - \frac{A_k}{2}\right)} + \frac{c_k^-}{s - i\left(\omega_k + \frac{A_k}{2}\right)} \right]. \tag{59}$$

C. Lamb shift and rotating frame

The effect of $\Sigma^{(2)}$ on $\langle S^+(t)\rangle$ was studied extensively in Ref. 9, where it was shown that it leads to both a shift in the precession frequency of the electron spin (Lamb shift) as well as a small decay of $\langle S^+(t)\rangle$ at short times, referred to as "visibility loss." In the limit of large N, the visibility loss effect is suppressed,[9,28] and one can make the approximation that the only role of the second-order memory kernel is to generate the Lamb shift. We will refer to this as the "Lamb shift approximation."

To make the definition of the Lamb shift more precise, first recall the Bromwich integral formula from Eq. (37):

$$\langle S^+(t)\rangle = \frac{\langle S^+(t=0)\rangle}{2\pi i} \int_{\gamma-i\infty}^{\gamma+i\infty} ds\, e^{st} \frac{1}{s - i\Omega_n + i\Sigma(s)}. \tag{60}$$

Since $\Sigma(s)$ vanishes at zero hyperfine coupling, it is clear from this formula that the zeroth-order behavior of $\langle S^+(t)\rangle$ is just a precession with frequency Ω_n. At nonzero coupling, this precession is shifted by an amount determined by the real part of the memory kernel. We define the Lamb shift $\Delta\Omega$ as the shift in precession frequency that would occur if the imaginary part of the memory kernel (the part which produces decay) were zero. We can read off a self-consistent equation for $\Delta\Omega$ from Eq. (60) by supposing $\mathrm{Im}[\Sigma(s)] = 0$ and requiring that the integrand have a pole at $s = i(\Omega_n + \Delta\Omega)$:

$$\Delta\Omega = -\mathrm{Re}[\Sigma(i\Omega_n + i\Delta\Omega)]. \tag{61}$$

In our flip-flop expansion, this can be approximated by

$$\Delta\Omega \approx -\mathrm{Re}[\Sigma^{(2)}(i\Omega_n + i\Delta\Omega)]. \tag{62}$$

Using this formula in conjuction with Eq. (59), we then find that the Lamb shift is given by

$$\Delta\Omega \approx \frac{1}{4\Omega_n} \sum_k A_k^2 (c_k^+ + c_k^-) \tag{63}$$

in the limit $\Omega_n \gg \omega_k, A_k$.

Now that we have defined the Lamb shift more precisely, we should also clarify the manner in which the Lamb shift approximation is implemented. This approximation consists of replacing $\Sigma^{(2)}(s + i\Omega_n + i\Delta\Omega) \to -\Delta\Omega$ in the expansion of the memory kernel. In order to make this replacement in (60), we need to shift the integration variable $s \to s + i\Omega_n + i\Delta\Omega$. In the Lamb shift approximation, we then have

$$\langle S^+\rangle = \frac{\langle S^+(t=0)\rangle}{2\pi i} e^{i(\Omega_n + \Delta\Omega)t} \int_{\gamma-i\infty}^{\gamma+i\infty} ds\, e^{st} \frac{1}{s + i\widetilde{\Sigma}^{(4)}(s)}, \tag{64}$$

where we have kept up to fourth order in the memory kernel and defined

$$\widetilde{\Sigma}^{(4)}(s) \equiv \Sigma^{(4)}(s + i\Omega_n + i\Delta\Omega). \tag{65}$$

It is often useful[28] to remove the high-frequency oscillations arising from the prefactor $e^{i(\Omega_n + \Delta\Omega)t}$ in Eq. (64) by introducing a "corotating" coherence measure x:

$$x(t) \equiv 2e^{-i(\Omega_n + \Delta\Omega)t} \langle S^+(t)\rangle. \tag{66}$$

Note that $\widetilde{\Sigma}^{(4)}(s)$ is the fourth-order term of the Laplace transform of the memory kernel in the rotating frame:

$$\widetilde{\Sigma}(t) = e^{-i(\Omega_n + \Delta\Omega)t} \Sigma(t). \tag{67}$$

This quantity serves as the kernel in the integro-differential equation governing the evolution of $x(t)$:

$$\dot{x}(t) = -i\Delta\Omega x(t) - i\int_0^t dt'\, \widetilde{\Sigma}(t-t')x(t'). \tag{68}$$

The rotating frame renders some of the more subtle features arising from the hyperfine flip-flops more transparent, and we will make extensive use of it when we solve the uniform coupling model using the NZ GME later on.

D. Fourth-order memory kernel

The fourth-order terms which emerge from inserting Eq. (42) into Eq. (46) are

$$\Sigma^{(4)}(s) = i\mathrm{Tr}\{S^+ P[1 - iL_0 QG_Q(s)]L_V QG_Q(s)L_V Q \\ \times G_Q(s)L_V QG_Q(s)QL_V PS^- \rho_I(0)\}. \tag{69}$$

We can again use Eq. (45) to replace $QG_Q(s)$ with $QG(s)$ and to discard most of the projection operators, yielding

$$\Sigma^{(4)}(s) = i\mathrm{Tr}\{S^+[1 - iL_0 QG(s)]L_V G(s)L_V Q \\ \times G(s)L_V G(s)L_V S^- \rho_I(0)\}. \tag{70}$$

If we then replace each instance of the propagator $G(s)$ with $\int_0^\infty dt\, e^{-st}G(t)$, then the remaining steps can be performed in a manner quite similar to the treatment we have given for the second-order memory kernel. This time, however, the expressions are much more complicated, and we relegate them to Appendix A.

E. High-frequency limit

From the explicit expression for the fourth-order memory kernel given in Appendix A, it is clear that the dominant contribution will come from the region $s \approx -i\Omega_n$. This is because the fourth-order memory kernel is a sum of many terms where each term is a product of three simple poles. Some of these poles are located at values of s which depend only on the kth nuclear Zeeman energy and hf coupling. However, most of the terms contain a pole located in the vicinity of $s \approx -i\Omega_n$. Due to this structure, $x(s)$ has poles at both $s \approx -i\Omega_n$ and at low frequencies, but the residues at the latter poles are strongly suppressed compared to the former ones. This means that if we consider the function $\bar{\Sigma}^{(4)}(s) \equiv \Sigma^{(4)}(s + i\Omega_n)$, we can neglect s, ω_k, and A_k relative to Ω_n. The resulting approximate expression for $\bar{\Sigma}^{(4)}(s)$ is given in Appendix A. The approximate expression for $\bar{\Sigma}^{(4)}(s)$

can be simplified by using the results of Appendix B to evaluate bath correlators, with the result

$$
\bar{\Sigma}^{(4)} \approx \frac{-i}{16\Omega_n^2} \sum_{k \neq \ell} A_k^2 A_\ell^2 \sum_i \rho_{ii} c_k^{(i)-} c_\ell^{(i)+} \frac{2s + i(A_k - A_\ell)}{s + i(A_k - A_\ell)}
$$

$$
\times \left\{ \frac{1}{s - i[\omega_k - \omega_\ell - \frac{1}{2}(A_k - A_\ell)]} \right.
$$

$$
\left. + \frac{1}{s + i[\omega_k - \omega_\ell + \frac{1}{2}(A_k - A_\ell)]} \right\}
$$

$$
- \frac{i}{16\Omega_n^2 s} \sum_i \rho_{ii} \left(\sum_k A_k^2 [c_k^{(i)-} + c_k^{(i)+}] \right)^2
$$

$$
+ \frac{i}{16\Omega_n^2 s} \left(\sum_k A_k^2 [c_k^- + c_k^+] \right)^2. \tag{71}
$$

The symbols $c_k^{(i)\pm}$ are defined in Appendix B. The fourth-order memory kernel given in Eq. (71) simplifies considerably if we assume a uniformly polarized nuclear bath. In this case, the last two terms in Eq. (71) cancel each other. This follows from the fact that $\sum_i \rho_{ii} c_k^{(i)\pm} c_\ell^{(i)\pm} = c^\pm c^\pm$ for such a bath; this identity is proven in Appendix B. (Here, $c_k^\pm = c^\pm$ is independent of k by definition.) In using this form of the identity, we are also assuming a homonuclear bath since we have thrown away the species information in discarding the site indices k and ℓ. This assumption could easily be lifted by introducing additional indices, but we will not do this for the sake of simplicity. Therefore, for a uniformly polarized homonuclear spin bath, we have

$$
\bar{\Sigma}^{(4)} \approx \frac{-i c^+ c^-}{4\Omega_n^2} \sum_{k \neq \ell} \frac{A_k^2 A_\ell^2}{s + i(A_k - A_\ell)}. \tag{72}
$$

Implementing the same procedure for obtaining the high-frequency limit on the second-order memory kernel, Eq. (59), we find that the result is a constant:

$$
\bar{\Sigma}^{(2)} \approx -\frac{c^+ + c^-}{4\Omega_n} \sum_k A_k^2 \approx -\Delta\Omega. \tag{73}
$$

In the last equality, we have pointed out that the high-frequency limit of $-\bar{\Sigma}^{(2)}$ is just the Lamb shift we have already computed. This was given in Eq. (63) in the context of a more general bath (not necessarily uniformly polarized). We see that the Lamb shift approximation is automatically incorporated into the high-frequency approximation.

V. THE NZ SOLUTION FOR THE UNIFORM COUPLING MODEL

We proceed to solve the uniform coupling model within the NZ framework in the case where all nuclei have spin 1/2. We will find that the solution is structurally incompatible with the exact solution reviewed in Sec. III, except at very early times. Let us define the characteristic time

$$
\tau \equiv 4\frac{\Omega_n}{\mathcal{A}} \frac{N}{\mathcal{A}}. \tag{74}
$$

Note that $\tau \approx \Delta\Omega^{-1}$. For times $t \lesssim \tau$, the NZ solution agrees quite well with the exact solution; however, we will show that

beyond this time scale, the NZ result rapidly breaks down. We will argue that this failure is an unavoidable consequence of the basic structure of the perturbative NZ approach with projector as defined in Eq. (31), suggesting that this approach is inappropriate in the case at hand. A remedy for this problem will be presented in Sec. V C.

Starting from the expressions for the second- and fourth-order memory kernels, Eqs. (59) and (A21), assuming a homonuclear bath, $\omega_k = \omega$, and setting $A_k = A = \mathcal{A}/N$, we find in the rotating frame

$$
\widetilde{\Sigma}^{(2)} = -\frac{i\mu c^-}{s + i\varpi_1} - \frac{i\mu c^+}{s + i\varpi_2}, \tag{75}
$$

$$
\widetilde{\Sigma}^{(4)} = \left[\frac{1}{s + i\varpi_1} + \frac{1}{s + i\varpi_2} \right]^2 \left[\frac{2i\mu^2 c^+ c^-}{s + i\varpi_3} + \frac{i\mu^2 c^+ c^-}{s + i\varpi_4} \right], \tag{76}
$$

with

$$
\begin{aligned}
\varpi_1 &= \Omega_n + \Delta\Omega - \omega - \mathcal{A}/(2N), \\
\varpi_2 &= \Omega_n + \Delta\Omega - \omega + \mathcal{A}/(2N), \\
\varpi_3 &= 2\Omega_n - 2\omega + \Delta\Omega, \\
\varpi_4 &= \Delta\Omega,
\end{aligned} \tag{77}
$$

and

$$
\mu \equiv \frac{\mathcal{A}^2}{4N} = \frac{\Omega_n}{\tau}. \tag{78}
$$

In the limit of uniform couplings with spin-1/2 nuclei, the Lamb shift reduces to

$$
\Delta\Omega \approx \frac{\mathcal{A}^2}{4N\Omega_n} = \frac{\mu}{\Omega_n}. \tag{79}
$$

In the above results, we have used the fact that we are restricting to the case of a uniformly polarized nuclear bath so that the bath correlators $c_k^\pm = c^\pm$ are independent of the nuclear site index k. Further details about how the dependence on $c^\pm$ arises in (75) and (76) are given in Appendix B. For the remainder of this section, we will absorb ω into the definition of Ω_n. In the rotating frame, $x(t)$ must depend on ω only in the combination $\Omega - \omega$, so it is simple to restore the explicit ω dependence if desired. In any case, it is generally safe to neglect ω since for any finite magnetic field $\omega \ll \Omega$.

The solution to Eq. (68) for the electron spin coherence $x(t)$ in terms of a Bromwich inversion integral is

$$
x(t) = \frac{1}{2\pi i} \int_{\gamma - i\infty}^{\gamma + i\infty} ds\, e^{st} \frac{x_0}{s + i\Delta\Omega + i\widetilde{\Sigma}^{(2)}(s) + i\widetilde{\Sigma}^{(4)}(s)}, \tag{80}
$$

where $x_0 \equiv x(t = 0)$ is the initial condition in the time domain. Note that we are not making the Lamb shift approximation here since we are keeping the full $\widetilde{\Sigma}^{(2)}(s)$. The Laplace transform of $x(t)$ is a rational function:

$$
x(s) = x_0 \frac{R(s)}{\Phi(s)}, \tag{81}
$$

where the polynomials $R(s)$ and $\Phi(s)$ are given by

$$
R(s) \equiv (s + i\varpi_1)^2 (s + i\varpi_2)^2 (s + i\varpi_3)(s + i\varpi_4), \tag{82}
$$

$$\Phi(s) \equiv (s + i\Delta\Omega)R(s) + \mu c^- \frac{R(s)}{s + i\varpi_1} + \mu c^+ \frac{R(s)}{s + i\varpi_2}$$
$$- \mu^2 c^+ c^- [2s + i(\varpi_1 + \varpi_2)]^2 [3s + i\varpi_3 + 2i\varpi_4]. \tag{83}$$

The fact that $x(s)$ is a rational function guarantees that the sum of the residues equals x_0 so that x_0 is indeed the initial value of $x(t)$. Denoting the seven zeros of $\Phi(s)$ by s_i, we may write

$$\Phi(s) = \prod_{i=0}^{6} (s - s_i). \tag{84}$$

We can solve for the s_i perturbatively in the small parameter $\frac{\mathcal{A}^2}{N\Omega_n^2} \ll 1$ (equivalently, $\Omega_n\tau \gg 1$). This essentially amounts to an expansion in small μ about the zeros of $sR(s)$, which are 0, $-i\varpi_1$, $-i\varpi_2$, $-i\varpi_3$, and $-i\varpi_4$. Since $-i\varpi_1$ and $-i\varpi_2$ are each zeros of $sR(s)$ with multiplicity 2, they will each give rise to two separate zeros of $\Phi(s)$. We must also keep in mind that the Lamb shift is linear in μ [see Eq. (79)]. We have

$$\Phi(s) = \left(s + i\eta\frac{\mu}{\Omega_n}\right)R(s) + \eta\mu c^- \frac{R(s)}{s + i\varpi_1} + \eta\mu c^+ \frac{R(s)}{s + i\varpi_2}$$
$$- \mu^2 c^+ c^- [2s + i(\varpi_1 + \varpi_2)]^2 [3s + i\varpi_3 + 2i\varpi_4]. \tag{85}$$

We have also introduced the parameter η so that we may consider the effect of making the Lamb shift approximation, which would amount to neglecting both the $\Delta\Omega$ and $\widetilde{\Sigma}^{(2)}(s)$ (under the assumption that they cancel one another) in the denominator of Eq. (80). This approximation is implemented by setting $\eta = 0$.

Having introduced all the bookkeeping devices we will need, we can proceed to compute the zeros of $\Phi(s)$ approximately by finding the u_i which solve the equation

$$\Phi(s_{R,i} + \mu u_i) = 0 \tag{86}$$

to leading order in μ, where $s_{R,i}$ satisfies

$$s_{R,i} R(s_{R,i}) = 0, \tag{87}$$

Following this recipe, the s_i are found to be

$$s_0 = -i\frac{1}{2\tau}[1 + \sqrt{1 + 16c^+ c^-}],$$
$$s_1 = -i\frac{1}{2\tau}[1 - \sqrt{1 + 16c^+ c^-}],$$
$$s_2 = -i\varpi_1 + \frac{c^-}{2\tau}[-i\eta - \sqrt{4c^+/c^- - \eta}],$$
$$s_3 = -i\varpi_1 + \frac{c^-}{2\tau}[-i\eta + \sqrt{4c^+/c^- - \eta}], \tag{88}$$
$$s_4 = -i\varpi_2 + \frac{c^+}{2\tau}[-i\eta - \sqrt{4c^-/c^+ - \eta}],$$
$$s_5 = -i\varpi_2 + \frac{c^+}{2\tau}[-i\eta + \sqrt{4c^-/c^+ - \eta}],$$
$$s_6 = -i\varpi_3.$$

We have kept only up to first order in $\mathcal{A}^2/N\Omega_n^2 = (\Omega_n\tau)^{-1}$ in the above expressions for the s_i. Notice that $s_6 = -i\varpi_3$, so that this root of $\Phi(s)$ is also a root of $R(s)$ and thus is not a pole

of $x(s)$. The residues of $x(s)$ at the poles (s_i for $i = 0, \ldots, 5$) are $2\pi i r_i$ where

$$r_0 = \frac{x_0}{2}\left(-1 + \frac{\eta}{\Omega_n\tau}\right)\frac{1 - \sqrt{1 + 16c^+ c^-}}{\sqrt{1 + 16c^+ c^-}},$$
$$r_1 = \frac{x_0}{2}\left(1 - \frac{\eta}{\Omega_n\tau}\right)\frac{1 + \sqrt{1 + 16c^+ c^-}}{\sqrt{1 + 16c^+ c^-}},$$
$$r_2 = -ix_0\frac{c^-}{4\Omega_n\tau}\frac{(i\eta + \sqrt{4c^+/c^- - \eta})^2}{\sqrt{4c^+/c^- - \eta}},$$
$$r_3 = ix_0\frac{c^-}{4\Omega_n\tau}\frac{(-i\eta + \sqrt{4c^+/c^- - \eta})^2}{\sqrt{4c^+/c^- - \eta}}, \tag{89}$$
$$r_4 = -ix_0\frac{c^+}{4\Omega_n\tau}\frac{(i\eta + \sqrt{4c^-/c^+ - \eta})^2}{\sqrt{4c^-/c^+ - \eta}},$$
$$r_5 = ix_0\frac{c^+}{4\Omega_n\tau}\frac{(-i\eta + \sqrt{4c^-/c^+ - \eta})^2}{\sqrt{4c^-/c^+ - \eta}}.$$

The electron spin coherence in the rotating frame is then

$$x_{NZ}(t) = \sum_{i=0}^{5} r_i e^{s_i t}. \tag{90}$$

A. Time scale for validity of the NZ GME uniform coupling model solution

Notice that two of the exponentials contributing to $x(t)$ always diverge in the large-time limit. The terms associated with the poles s_3 and s_5 exhibit this divergence for nearly all nuclear polarizations. The only exception is the case of maximal polarization, for which $c^+ c^- = 0$; we will return to this special case shortly. The fact that divergences arise suggests that the NZ result for the uniform coupling model breaks down on a time scale given roughly by $\tau \sim N\Omega/\mathcal{A}^2$. The positive real parts of the s_i are direct contributions of the fourth-order memory kernel. Even though these contributions appear to introduce a time scale cutoff for the solution, their presence actually extends the validity of the NZ result to larger times, as will be shown in the next section when we compare the NZ solution with the exact solution.

Although the large-time divergences generated by the positive real parts of the s_i indicate that there must be a time scale cutoff, they are not really responsible for this cutoff. In particular, even if no divergences were present, the result we have obtained for $x(t)$ in the uniform coupling model would still be invalid beyond the time scale of τ. This is because we are solving perturbatively for the phases $\text{Im}(s_i)$ in the phase factors $\exp[i\text{Im}(s_i)t]$ appearing in Eq. (90). If we solved for $\text{Im}(s_i)$ to order $\mathcal{A}^2/N\Omega_n \sim 1/\tau$, then the result would be valid up to time scales which are inversely related to the next order in the flip-flop expansion ($t \sim N^2\Omega_n^3/\mathcal{A}^4$), since corrections to the periodic phase factor $\exp[i\text{Im}(s_i)t]$ resulting from a small correction δs_i will become significant when $\text{Im}(\delta s_i)t \sim 1$ regardless of the fact that $\mathcal{A}/\sqrt{N}\Omega_n \ll 1$. However, it is important to note that we have not obtained the full $O(\mathcal{A}^2/N\Omega_n)$ contributions to the s_i as is suggested by the particular form of the expressions given in Eq. (88). Specifically, if we focus only on the fourth-order memory

kernel contributions by setting $\eta = 0$, it is evident that the s_i still receive corrections at order $\mathcal{A}^2/N\Omega_n \sim 1/\tau$. Therefore, we see that higher-order terms in the flip-flop expansion modify the lowest-order corrections to the s_i, and we would need to include all terms in the expansion of the memory kernel in order to obtain the full $O(\mathcal{A}^2/N\Omega_n)$ corrections to the s_i. Of course, keeping all these terms would yield the exact s_i and r_i and not just the $O(\mathcal{A}^2/N\Omega_n)$ corrections. We conclude that the NZ approach with the simple projector defined in Eq. (31) and in which the memory kernel is computed up to some finite order in flip-flops will yield a solution for the uniform coupling model which is valid only up to the time scale of $t < \tau$. We have checked that even if one computes the poles of $\Phi(s)$ exactly (numerically), the NZ result still breaks down at the time scale $t \sim \tau$, in further support of the conclusion that the breakdown on this time scale can be avoided only by keeping higher-order terms in the memory kernel expansion.

A notable exception to the above argument arises in the case of maximal nuclear spin polarization $m = \pm N/2$, where either $c^+ = 0$ or $c^- = 0$. In this case, the fourth-order memory kernel vanishes identically and so does not modify the s_i, suggesting that the NZ result is valid on arbitrarily large time scales. We will see below that the NZ approach incorporating only the second-order memory kernel yields the exact solution[7,9] in this special case, confirming this conjecture.

Note that the above conclusions are compatible with the considerations of relevant time scales in a realistic, inhomogeneously coupled system. There we expect the box model to apply at short times, $t \ll N/\mathcal{A}$. The previous works applying the NZ theory to such a problem were focusing on the high-field regime, $\mathcal{A}/\Omega < 1$, in which the long-time solution could be controlled perturbatively. Under this condition, $\tau > N/\mathcal{A}$, and the NZ theory successfully describes the short-time coherence dynamics.[28] At low magnetic fields, however, we have $\tau < N/\mathcal{A}$, and the NZ approach is not expected to work properly at the short time scale.

B. Comparison with the exact solution

When the nuclear spin polarization is maximal, $m = \pm N/2$, the fourth-order memory kernel vanishes identically. For concreteness, we consider the case $m = N/2$ ($c^+ = 0$, $c^- = 1$), in which the Laplace transform of the spin coherence becomes quite simple:

$$x(s) = x_0 \frac{s + i\varpi_1}{s(s + i\varpi_1) + \mu}. \tag{91}$$

Since there are only two poles, we can obtain these exactly,

$$s_\pm = -i\frac{\varpi_1}{2} \pm \frac{i}{2}\sqrt{\varpi_1^2 + 4\mu}, \tag{92}$$

and it is likewise a simple matter to compute the residues:

$$2\pi i r_\pm = \frac{x_0}{2}\left[1 \pm \frac{\varpi_1}{\sqrt{\varpi_1^2 + 4\mu}}\right]. \tag{93}$$

The electron spin coherence is then given by

$$x(t) = \sum_\pm r_\pm e^{s_\pm t} = x_0 e^{-i\varpi_1 t/2}\left[\cos\left(\frac{t}{2}\sqrt{\varpi_1^2 + 4\mu}\right) + i\frac{\varpi_1}{\sqrt{\varpi_1^2 + 4\mu}}\sin\left(\frac{t}{2}\sqrt{\varpi_1^2 + 4\mu}\right)\right]. \tag{94}$$

Plugging in the expressions for ϖ_1 and μ, Eqs. (77) and (78), we obtain the exact solution from Eq. (25) with $m = N/2$. The fact that the second-order memory kernel suffices for obtaining the exact solution[7] for any distribution of A_k in the case of maximal polarization was previously pointed out in Ref. 9.

Returning to the case of arbitrary nuclear polarization m, it is straightforward to check that the NZ result agrees with the exact solution for short times. In particular, if we consider the case $t \ll \tau$, then we may approximate the poles as follows:

$$s_0 \approx s_1 \approx 0, \quad s_2 \approx s_3 \approx -i\varpi_1, \quad s_4 \approx s_5 \approx -i\varpi_2, \tag{95}$$

leading to the short-time behavior

$$x(t) \approx x_0 + \frac{x_0}{\Omega_n \tau}(c^- e^{-i\varpi_1 t} + c^+ e^{-i\varpi_2 t} - 1). \tag{96}$$

Now turning to the exact solution, Eq. (25), we can implement the same approximation by replacing $N_{jm}^+ \approx \varpi_2$, $N_{jm}^- \approx \varpi_1$ in the arguments of the sines and cosines arising from a_{jm}^* and c_{jm}. Furthermore, we expand the coefficients of the sines to second order in the hyperfine coupling:

$$\frac{Z_{jm}^+}{N_{jm}^+} \approx 1 - \frac{\mathcal{A}^2}{2\varpi_2^2 N^2}[j(j+1) - m(m+1)],$$

$$\frac{Z_{jm}^-}{N_{jm}^-} \approx 1 - \frac{\mathcal{A}^2}{2\varpi_1^2 N^2}[j(j+1) - m(m-1)]. \tag{97}$$

At least for low to moderate nuclear polarizations and considering that for typical values of j we may write $j(j+1) \sim N$, this approximation is valid roughly in the limit $\Omega \gg \mathcal{A}/\sqrt{N}$. In the above expressions, we can replace ϖ_1 and ϖ_2 with Ω_n since the differences lead to higher-order corrections in $\mathcal{A}/(\Omega N)$. After some algebra, we arrive at

$$x(t) \approx x_0\left\{1 - \frac{2}{\Omega_n \tau N Z}\sum_{j=|m|}^{N/2} n_j[j(j+1) - m^2]\right\}$$

$$+ \frac{x_0}{\Omega_n \tau N Z}e^{-i\varpi_2 t}\sum_{j=|m|}^{N/2} n_j[j(j+1) - m(m+1)]$$

$$+ \frac{x_0}{\Omega_n \tau N Z}e^{-i\varpi_1 t}\sum_{j=|m|}^{N/2} n_j[j(j+1) - m(m-1)]. \tag{98}$$

The identity

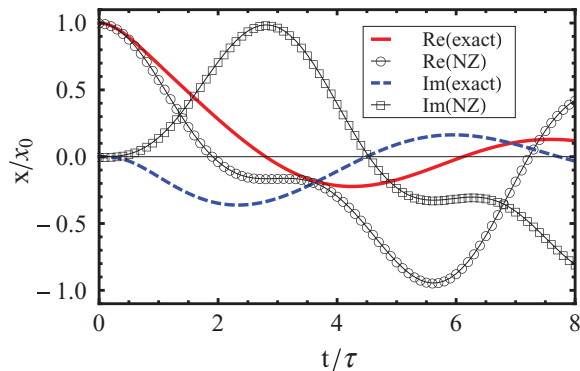$$\frac{2}{NZ}\sum_{j=|m|}^{N/2} n_j[j(j+1) - m^2] = 1 \tag{99}$$

FIG. 1. (Color online) Exact solution of the uniform coupling model [Eq. (25)] vs NZ GME result [Eq. (90)] for $\mathcal{A} = \Omega$, $\omega/\Omega = 10^{-3}$, and $m = 0$.

immediately implies that [using also Eq. (B7)]

$$\frac{1}{NZ} \sum_{j=|m|}^{N/2} n_j [j(j+1) - m^2 \pm m] = c^{\mp}, \qquad (100)$$

and we get back the short-time NZ result, Eq. (96).

In Fig. 1, we compare the NZ result with the exact solution in the case of zero net nuclear polarization ($m = 0$), and it is clear that the two agree only for short times $t \lesssim \tau/2$. We have not specified the number of nuclei in the caption of Fig. 1 because the curves are valid for a wide range of N. This is because the envelope of $x(t/\tau)$ is essentially independent of N, as can be seen by noticing that the envelope arises from the first two contributions, $r_0 e^{s_0 t} + r_1 e^{s_1 t}$, and these contributions depend on N only through their τ dependence. [In the case of very long times, the last four contributions to $x(t)$ become comparable to the first two, and all six terms generate the envelope, but this is well beyond the regime of validity, $t \lesssim \tau$, of the NZ GME result. Also note that in addition to the dependence of the first two contributions on N coming from τ, there is a weak N dependence coming from the $c^{\pm}$ factors in the case of nonzero and nonmaximal nuclear polarization as well.] The remaining four contributions to $x(t)$ give rise to a small modulation which is visible in Figs. 2 and 3. The frequency and amplitude of this modulation are given roughly by $\Omega_n \tau$ and $1/(\Omega_n \tau)$, respectively. Since $\Omega_n \tau = 4N\Omega_n^2/\mathcal{A}^2$, we see that the frequency scales linearly with N, while the amplitude scales as $1/N$. This behavior is evident in a comparison of Figs. 2 and 3.

It should be stressed that, while the value of $\mathcal{A}/\Omega$ plays a crucial role for the long-time results in the nonuniform coupling case,[9,28] this parameter does not have any particular significance in the uniform coupling case considered here. The amplitude of the fast oscillation in the exact and NZ results depends of course on the ratio of $\mathcal{A}/\Omega$, but for large N the amplitude of this oscillation does not become significant in the range of Ω which we consider, i.e., $\Omega \gg \mathcal{A}/\sqrt{N}$. On the other hand, the envelope of the NFID signal depends on Ω and $\mathcal{A}$ only through $\tau \approx (N/\mathcal{A})(\Omega/\mathcal{A})$. When the parameter $\mathcal{A}/\Omega$ is varied between 0.1 and 10, the envelopes in Fig. 1 do not change, only the fast-oscillation components change; the (dis)agreement between the NZ solution and the exact result remains unchanged.
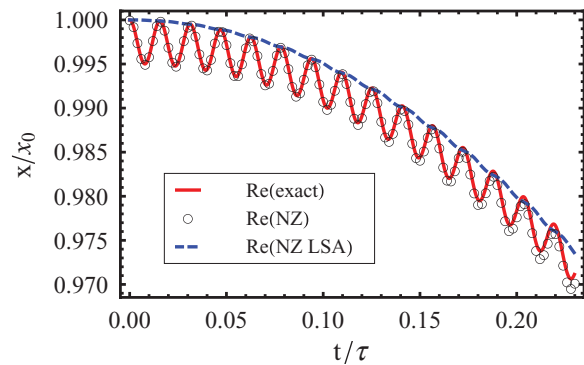

FIG. 2. (Color online) Zoomed-in version of Fig. 1 along with the Lamb shift approximation (LSA) of the NZ GME result for $N = 100$.

Both the envelope and modulation change under variations of the nuclear polarization m. The case $m = N/4$ is shown in Figs. 4 and 5. Figure 4 reveals that $m = N/4$ is in some sense special because the NZ approach is able to reproduce the oscillation period of the $x(t)$ envelope along with the amplitude of its real part. We have tried various nuclear polarizations and found that the NZ approach is able to reproduce these features only in the $m = N/4$ case. Generically, the single-projector NZ result visibly disagrees with the exact solution beyond $t \sim \tau$.

The fact that Figs. 1–5 show that the NZ solution, Eq. (90), disagrees with the exact answer in Eq. (25) beyond time $t \sim \tau$ is not surprising in light of the fact that the exact solution is a sum over a large number of oscillatory functions, while the NZ result consists of a sum of only six exponentials. In the case of a realistic wave function, the NZ approach can lead to more complicated behavior due to an appearance of branch cuts in the continuum limit[9,28] It is should also be strongly stressed that for a realistic wave function, a new pole related to flip-flops between nuclei with similar, but distinct, values of A_k, appears. In fact, this pole dominates the high-field and long-time decay of coherence, and its influence is well controlled for times much longer than τ and $T_2 \approx \tau(\frac{\Omega}{\mathcal{A}})$, as discussed in Ref. 28. This is in stark contrast to the behavior of a few poles determining the coherence dynamics in the uniform coupling case.
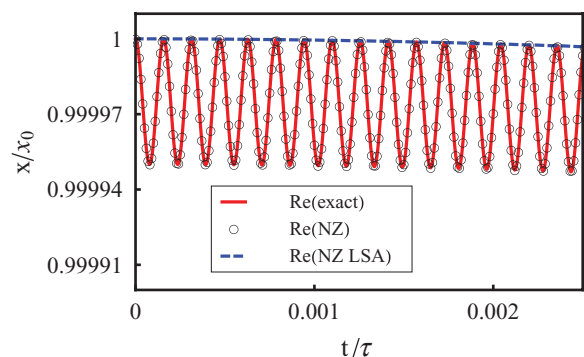

FIG. 3. (Color online) Zoomed-in version of Fig. 1 along with the Lamb shift approximation (LSA) of the NZ GME result for $N = 10^4$.
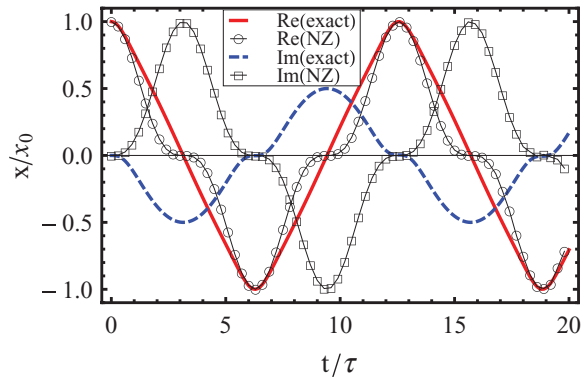
FIG. 4. (Color online) Exact solution of the uniform coupling model [Eq. (25)] vs. NZ GME result [Eq. (90)] for $N = 10^4$, $\mathcal{A} = \Omega$, $\omega/\Omega = 10^{-3}$ and $m = N/4$.

C. The NZ solution of the uniform coupling model using correlated projectors

We have seen that a straightforward application of the standard NZ GME to the uniform coupling model yields a result which is in good agreement with the exact solution only for very short times. From the technical point of view, this failure of the NZ approach could be traced back to not having enough poles in the Laplace-transformed solution, i.e., not having enough frequencies to sum over in the real-time expression. Clearly, in order to reproduce the exact answer one needs to find a way of bringing all these missing frequencies back into the theory.

The above NZ results were obtained using a standard choice for the projection operator P, which was defined in Eq. (31). However, it was shown in Ref. 22 that the standard projection operator is far from being the best possible choice in contexts where the Hamiltonian exhibits a significant degree of symmetry. When symmetries are present, one can instead replace P with a series of so-called *correlated* projection operators which project onto invariant subspaces of state space, enabling one to expand the reduced density matrix for the system as a sum of matrices, each capturing the components of the state lying in a particular subspace. This greatly enhances the number of dynamical degrees of freedom, resulting in a remarkable improvement in the agreement between the NZ
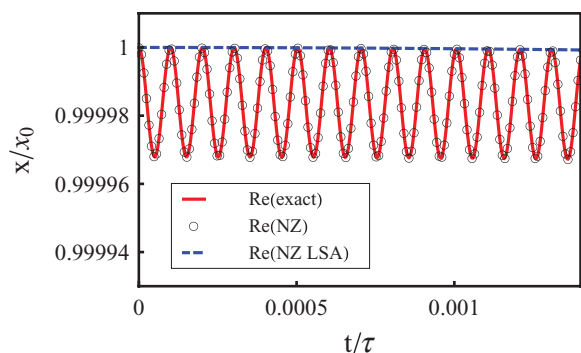

FIG. 5. (Color online) Zoomed-in version of Fig. 4 along with the Lamb shift approximation (LSA) of the NZ GME result for $N = 10^4$.

calculation and the exact result. In this section we will show that, whereas the standard fourth-order NZ result agrees rather poorly with the exact solution, even at second order the NZ GME agrees extremely well with the exact answer when correlated projectors are employed.

For this calculation, we choose to work in the interaction picture defined with respect to the unperturbed (Zeeman and Overhauser) part of the Hamiltonian, H_0. In terms of the Liouville operator L_I and total density matrix $\tilde{\rho}$ in the interaction picture, the second-order NZ GME equation for the electron spin coherence $\tilde{\rho}_{e,-+}$ becomes

$$\dot{\tilde{\rho}}_{e,-+} = -\int_0^t dt' \text{Tr}\{S^+ P L_I(t) L_I(t') P \tilde{\rho}(t')\}. \quad (101)$$

For the uniform coupling model, L_I acts on an arbitrary density matrix as

$$
L_I \begin{pmatrix} \rho_{++} & \rho_{+-} \\ \rho_{-+} & \rho_{--} \end{pmatrix}
$$
$$
= \frac{1}{2} \begin{pmatrix} h_{+-}\rho_{-+} - \rho_{+-}h_{-+} & h_{+-}\rho_{--} - \rho_{++}h_{+-} \\ h_{-+}\rho_{++} - \rho_{--}h_{-+} & h_{-+}\rho_{+-} - \rho_{-+}h_{+-} \end{pmatrix},
$$
$$(102)$$

with

$$
\begin{aligned}
h_{+-} &\equiv (\mathcal{A}/N)e^{i(\Omega - \mathcal{A}/(2N))t} I^- e^{i(\mathcal{A}/N)t I^z}, \\
h_{-+} &\equiv (\mathcal{A}/N)e^{-i(\Omega + \mathcal{A}/(2N))t} I^+ e^{-i(\mathcal{A}/N)t I^z} = h^\dagger_{+-},
\end{aligned}
\quad (103)
$$

where $I^\pm = \sum_k I_k^\pm$ are the total nuclear creation and annihilation operators. At this point, we are ready to define the correlated projection operators appropriate for the uniform coupling model. In Sec. III, we already made use of the fact that in the case of uniform couplings, the total nuclear angular momentum is conserved, and we may work in the $|jm\rangle$ basis of nuclear states. Defining the nuclear operator Π_{jm} to be the projector onto the subspace of fixed j and m quantum numbers, we choose the superprojector P to be such that it acts on the total density matrix as[22]

$$
P\tilde{\rho} = \sum_{jm} \text{Tr}_I(\Pi_{jm}\tilde{\rho}) \otimes \frac{1}{n_j}\Pi_{jm} \equiv \sum_{jm} \tilde{\rho}_e^{jm} \otimes \frac{1}{n_j}\Pi_{jm}. \quad (104)
$$

The $\tilde{\rho}_e^{jm}$ are a set of matrices which sum to give the reduced density matrix for the electron spin:

$$
\tilde{\rho}_e = \sum_{jm} \tilde{\rho}_e^{jm} = \sum_{m=-N/2}^{N/2} \sum_{j=|m|}^{N/2} n_j \tilde{\rho}_e^{jm}. \quad (105)
$$

Inserting Eq. (104) into Eq. (101), we obtain after some algebra

$$
\begin{aligned}
\dot{\tilde{\rho}}_{e,-+}^{jm}(t) = -\frac{1}{4}\int_0^t dt' [&e^{-i Z_m^+(t-t')}(X_{jm}^+)^2 \\
&+ e^{i Z_m^-(t-t')}(X_{jm}^-)^2]\tilde{\rho}_{e,-+}^{jm}(t'),
\end{aligned}
\quad (106)
$$

where $X_{jm}^\pm$ and $Z_m^\pm$ were defined earlier in Eq. (21). Taking the Laplace transform of both sides of Eq. (106), we obtain an algebraic equation for the Laplace transform of

$\tilde{\rho}_{e,-+}^{jm}(t)$ [which we call $\tilde{\rho}^{jm}(s)$ for brevity] which is readily solved:

$$\tilde{\rho}^{jm}(s) = \rho_0^{jm}(s + i Z_m^+)(s - i Z_m^-)\Big\{ s^3 + i(Z_m^+ - Z_m^-)s^2$$

$$+ \Big[Z_m^+ Z_m^- + \frac{1}{4}(X_{jm}^+)^2 + \frac{1}{4}(X_{jm}^-)^2 \Big] s$$

$$+ \frac{i}{4}[Z_m^+(X_{jm}^-)^2 - Z_m^-(X_{jm}^+)^2] \Big\}^{-1}. \quad (107)$$

ρ_0^{jm} is the intial value of $\tilde{\rho}_{e,-+}^{jm}(t)$. To obtain $\tilde{\rho}_{e,-+}^{jm}(t)$, we must use the Bromwich inversion formula:

$$\tilde{\rho}_{e,-+}^{jm}(t) = \frac{\rho_0}{2\pi i} \lim_{\gamma \to 0} \int_{\gamma - i\infty}^{\gamma + i\infty} ds \, e^{st} \tilde{\rho}^{jm}(s). \quad (108)$$

The value of this integral is determined by the three poles of $\tilde{\rho}^{jm}(s)$, which we will call $s_1^{jm}, s_2^{jm}, s_3^{jm}$, and by their associated residues $r_1^{jm}, r_2^{jm}, r_3^{jm}$. In terms of these poles, the solution is

$$\tilde{\rho}_{e,-+}^{jm}(t) = \rho_0^{jm} \sum_{i=1}^{3} r_i^{jm} e^{s_i^{jm} t}, \quad (109)$$

where the residues are given by

$$r_1^{jm} = \frac{(s_1^{jm} + i Z_m^+)(s_1^{jm} - i Z_m^-)}{(s_1^{jm} - s_2^{jm})(s_1^{jm} - s_3^{jm})},$$

$$r_2^{jm} = \frac{(s_2^{jm} + i Z_m^+)(s_2^{jm} - i Z_m^-)}{(s_2^{jm} - s_1^{jm})(s_2^{jm} - s_3^{jm})}, \quad (110)$$

$$r_3^{jm} = \frac{(s_3^{jm} + i Z_m^+)(s_3^{jm} - i Z_m^-)}{(s_3^{jm} - s_1^{jm})(s_3^{jm} - s_2^{jm})}.$$

To complete the solution, we must give the explicit forms of the s_i^{jm}:

$$s_1^{jm} = -\frac{a}{3} - \frac{2^{1/3}}{3d}(3b - a^2) + \frac{d}{2^{1/3}3},$$

$$s_2^{jm} = -\frac{a}{3} + \frac{(1 + i\sqrt{3})(3b - a^2)}{2^{2/3}3d} - \frac{(1 - i\sqrt{3})d}{2^{1/3}6}, \quad (111)$$

$$s_3^{jm} = -\frac{a}{3} + \frac{(1 - i\sqrt{3})(3b - a^2)}{2^{2/3}3d} - \frac{(1 + i\sqrt{3})d}{2^{1/3}6},$$

with

$$d \equiv (-2a^3 + 9ab - 27c$$
$$+ 3\sqrt{3}\sqrt{-a^2b^2 + 4b^3 + 4a^3c - 18abc + 27c^2})^{1/3}, \quad (112)$$

and

$$a = i(Z_m^+ - Z_m^-),$$

$$b = Z_m^+ Z_m^- + \frac{1}{4}(X_{jm}^+)^2 + \frac{1}{4}(X_{jm}^-)^2, \quad (113)$$

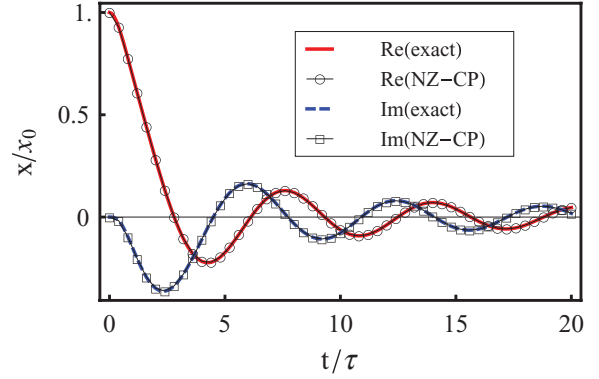$$c = \frac{i}{4}[Z_m^+(X_{jm}^-)^2 - Z_m^-(X_{jm}^+)^2].$$

FIG. 6. (Color online) Exact solution of the uniform coupling model [Eq. (25)] vs NZ-CP result [Eq. (114)] for $N = 10^4$, $\mathcal{A} = \Omega$, $\omega/\Omega = 10^{-3}$, and $m = 0$.

Since the interaction picture can be thought of as the frame rotating with frequency Ω_n, to switch to the rotating frame with frequency $\Omega_n + \Delta\Omega$ we simply need to multiply the result by $e^{-i\Delta\Omega t}$. The electron spin coherence in the rotating frame and in the presence of fixed nuclear polarization m is then

$$x_{\text{NZ-CP}}(t) = \frac{x_0}{Z} e^{-i\Delta\Omega t} \sum_{j=|m|}^{N/2} n_j \sum_{i=1}^{3} r_i^{jm} e^{s_i^{jm} t}. \quad (114)$$

This solution is plotted along with the exact solution in Figs. 6 and 7. It is clear from these figures that the NZ solution with correlated projectors (NZ-CP) agrees remarkably well with the exact solution.

It is not difficult to extract analytically the envelope and modulation from the NZ-CP solution. To do this, it helps to first perform a large-N expansion, wherein the leading-order terms in the s_i^{jm} are

$$s_1^{jm} \approx i Z_m^- - i\frac{(X_{jm}^-)^2}{4\Omega_n},$$

$$s_2^{jm} \approx i\frac{(X_{jm}^+)^2 + (X_{jm}^-)^2}{4\Omega_n}, \quad (115)$$

$$s_3^{jm} \approx -i Z_m^+ - i\frac{(X_{jm}^+)^2}{4\Omega_n},$$
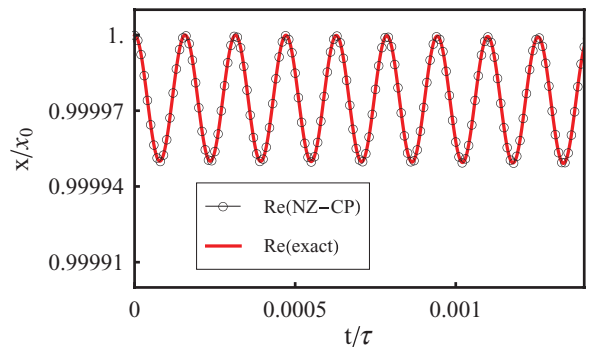

FIG. 7. (Color online) Zoomed-in version of Fig. 6.

while those of the r_i^{jm} are

$$r_1^{jm} \approx \frac{(X_{jm}^-)^2}{4\Omega_n^2},$$

$$r_2^{jm} \approx 1 - \frac{(X_{jm}^+)^2 + (X_{jm}^-)^2}{4\Omega_n^2}, \qquad (116)$$

$$r_3^{jm} \approx \frac{(X_{jm}^+)^2}{4\Omega_n^2}.$$

In the limit of large N, the coherence therefore takes the form

$$x_{\text{NZ-CP}}(t)$$

$$\approx \frac{x_0}{Z} e^{-i\Delta\Omega t} \sum_{j=|m|}^{N/2} n_j e^{i[(X_{jm}^+)^2 + (X_{jm}^-)^2]/4\Omega_n t}$$

$$\times \left\{ 1 - \frac{(X_{jm}^+)^2 + (X_{jm}^-)^2}{4\Omega_n^2} + \frac{(X_{jm}^+)^2}{4\Omega_n^2} \right.$$

$$\left. \times e^{-i[Z_m^+ + (X_{jm}^+)^2/4\Omega_n]t} + \frac{(X_{jm}^-)^2}{4\Omega_n^2} e^{-i[-Z_m^- + (X_{jm}^-)^2/4\Omega_n]t} \right\}.$$

$$(117)$$

The factor in curly brackets in Eq. (117) is precisely that which gives rise to the small modulation depicted in Fig. 7, while the rest of the expression produces the envelope in Fig. 6.

The above expression can be obtained from the exact solution, Eq. (25), by expanding in the limit $X_{jm}^\pm \ll Z_m^\pm$, in which case we find

$$a_{jm}^* \approx e^{i(N_{jm}^+/2)t} \left[1 - \frac{(X_{jm}^+)^2}{4(Z_m^+)^2}(1 - e^{-iN_{jm}^+ t}) \right],$$

$$c_{jm} \approx e^{i(N_{jm}^-/2)t} \left[1 - \frac{(X_{jm}^-)^2}{4(Z_m^-)^2}(1 - e^{-iN_{jm}^- t}) \right], \qquad (118)$$

where a_{jm}, c_{jm}, and $N_{jm}^\pm$ were defined in Eqs. (20) and (21). These expressions result from expanding only the $Z_m^\pm/N_{jm}^\pm$ factors appearing in a_{jm} and c_{jm}. If we furthermore expand the $N_{jm}^\pm$ factors in the temporal exponents as

$$N_{jm}^\pm \approx |Z_m^\pm| + \frac{(X_{jm}^\pm)^2}{4|Z_m^\pm|}, \qquad (119)$$

and also make the following approximation in the denominators:

$$Z_m^\pm \approx \Omega_n, \qquad (120)$$

then we get back Eq. (117).

If we assume typical values of j and m with $j \gg m$, then we have roughly $X_{jm}^\pm \sim \mathcal{A}/\sqrt{N}$, and the above approximations are valid in the limit $\Omega \gg \mathcal{A}/\sqrt{N}$. Recall that this is the same condition we had for the validity of the NZ solution without correlated projectors. In fact, the approximations we have made in the exact solution to arrive at the NZ-CP result are essentially the same ones we made to relate the exact and NZ solutions [see Eq. (97)], the only difference being that here we have kept some of the j dependence in the exponents when evaluating the sum over j. Moreover, note that the expansion of the $N_{jm}^\pm$ factor appearing in the temporal exponent of the exact solution introduces a time scale on which the solution is

valid. It is somewhat difficult to say precisely what the time scale of validity is, however, because of the sum over j. To obtain a very rough estimate, we can again consider a typical value of j and write $X_{jm}^\pm \sim \mathcal{A}/\sqrt{N}$. The time scale should roughly correspond to the inverse of the error introduced by expanding $N_{jm}^\pm$ in the temporal exponent. This error is on the order of

$$N_{jm}^\pm - |Z_m^\pm| - \frac{(X_{jm}^\pm)^2}{4|Z_m^\pm|} \sim \frac{(X_{jm}^\pm)^4}{|Z_m^\pm|^3} \sim \frac{\mathcal{A}^4}{N^2\Omega^3} \qquad (121)$$

(assuming that $j \gg m$), indicating a time scale

$$t \sim \frac{N^2\Omega^3}{\mathcal{A}^4}. \qquad (122)$$

D. Comparison with the RDT solution of the uniform coupling model

We now review the effective-Hamiltonian RDT solution to the box model and show how it is related to the exact solution and the NZ-CP result of the previous section. At second order in the flip-flop expansion, we have processes in which the electron spin flip-flops with the kth nucleus and then subsequently flip-flops with the ℓth nucleus. This leads to an effective flip-flop interaction between the kth and ℓth nuclear spins which is mediated by the hyperfine interaction. We can derive the effective Hamiltonian describing this internuclear flip-flop process by performing a canonical transformation on the hyperfine Hamiltonian in Eqs. (2)–(5): $H_{\text{eff}} = e^{-\mathcal{S}} H e^{\mathcal{S}}$, where the unitary operator $e^{-\mathcal{S}}$ is chosen in such a way as to eliminate the original V_{ff} interaction.[11,12,23,26] It is important to note that the transformation on states, $|\psi\rangle \rightarrow e^{-\mathcal{S}}|\psi\rangle$, is neglected in the derivation of H_{eff}. The dominant terms in the resulting effective Hamiltonian are

$$H_{\text{eff}} = -\sum_k \frac{A_k^2}{4\Omega} I_k^z + S^z \sum_k \frac{A_k^2}{2\Omega} \left[I_k^2 - (I_k^z)^2 \right]$$

$$+ S^z \sum_{k \neq \ell} \frac{A_k A_\ell}{2\Omega} I_k^+ I_\ell^-. \qquad (123)$$

The effective-Hamiltonian solution for NFID was obtained in Ref. 26 in the case of zero nuclear polarization, $m = 0$. In the rotating frame, it is given by

$$x(t) = x_0 e^{-i\Delta\Omega t} \frac{\exp[i \arctan(t/\tau)]}{\sqrt{1 + (t/\tau)^2}} = \frac{x_0 e^{-i\Delta\Omega t}}{1 - it/\tau}. \qquad (124)$$

This result is compared with the exact solution, Eq. (25), in Figs. 8 and 9. To generate these figures, we have used the high-frequency form of the Lamb shift, Eq. (63), where for zero polarization, $c_k^\pm = 1/2$ (see Appendix B). It is clear from Fig. 8 that the envelope of the RDT solution agrees very well with that of the exact solution up to time scales well beyond τ. The fact that the two envelopes agree even at very large time scales is particularly interesting given that, in the case of RDT, $x \sim 1/t$ for $t \gg \tau$; this $1/t$ tail is evidently reproduced by the sum of many exponential terms comprising the exact solution. On the other hand, Fig. 9 reveals that RDT does not succeed in capturing the fast small-amplitude modulation of the coherence.
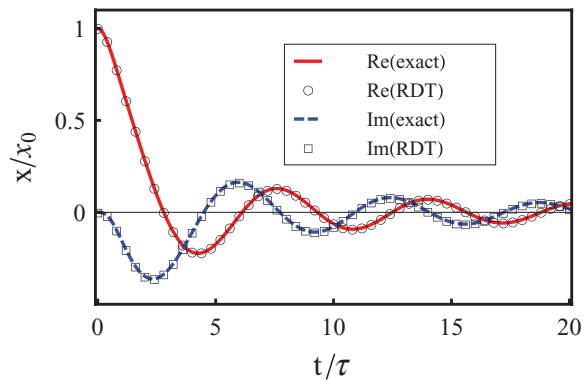
FIG. 8. (Color online) Exact solution of the uniform coupling model [Eq. (25)] vs RDT result [Eq. (124)] for $N = 10^4$, $\mathcal{A} = \Omega$, $\omega/\Omega = 10^{-3}$, and $m = 0$.

It is not difficult to extract the RDT solution as a limit of the exact solution. First recall that the RDT result using the effective Hamiltonian is expected to be valid[26] for $\Omega \gg \mathcal{A}/\sqrt{N}$ and in the limit of large N. Starting from the exact solution, Eq. (25), we can apply the first of these approximations along with the fact that for the j states which contribute the most to the sums we have $j(j + 1) \sim N$, to write

$$Z_m^\pm \approx \pm \Omega, \quad N_{jm}^\pm \approx \Omega \left[1 + \frac{\mathcal{A}^2}{2\Omega^2 N^2} j(j + 1) \right], \quad (125)$$

so that we obtain

$$x(t) \approx x_0 e^{-i\Delta\Omega t} \frac{1}{Z} \sum_{j=0}^{N/2} n_j e^{i(2/N)j(j+1)t/\tau}. \quad (126)$$

Expanding the exponential and using the result that in the large-N limit

$$\frac{1}{Z} \sum_{j=0}^{N/2} n_j j^k (j + 1)^k = \frac{k! N^k}{2^k} + O(N^{k-1}), \quad (127)$$

we arrive at the RDT solution:

$$x(t) \approx x_0 e^{-i\Delta\Omega t} \sum_{k=0}^{\infty} \left(\frac{it}{\tau} \right)^k = \frac{x_0 e^{-i\Delta\Omega t}}{1 - it/\tau}. \quad (128)$$

Strictly speaking, this derivation is valid only for $t < \tau$ since otherwise the infinite series in Eq. (128) is not defined, and the last line in Eq. (128) should be treated as an analytical
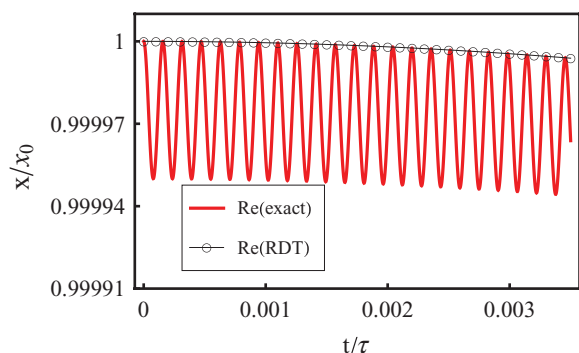

FIG. 9. (Color online) Zoomed-in version of Fig. 8.

continuation of the previous expression along the real axis (a similar kind of analytical continuation was in fact encountered in the derivation of the RDT result in Ref. 26). The correctness of the analytical continuation can be easily checked by comparing a numerical evaluation of Eq. (126) with Eq. (124) in the limit $N \to \infty$ for all times t.

Notice that the approximations we have made in the exact solution to arrive at the RDT result are essentially the same ones we made to relate the exact and NZ-CP solutions [see Eq. (119)], the only difference being that in the context of NZ-CP, we kept one more order in the expansion, yielding the additional factor in curly brackets in Eq. (117). This additional factor is precisely that which gives rise to the small modulation depicted in Fig. 7. Thus, the RDT and NZ-CP solutions of the box model belong to the same expansion of the exact solution. Moreover, note that it is the expansion of the $N_{jm}^\pm$ factor appearing in the temporal exponent of the exact solution that introduces a time scale on which the NZ-CP solution is valid. The fact that we are making the very same expansion here implies that the RDT solution will be valid on a time scale similar to that of the NZ-CP result.

VI. DISCUSSION

In this section, we aim to understand the reasons for the failure of the standard (single-projector) NZ approach discussed in Sec. V and for the success of the correlated projector approach from the previous section.

A. Non-narrowed Gaussian bath

It is instructive to take a small detour, and discuss first the NZ solution for the case of Ising coupling to the bath spins,[59] for which $V_{ff} = 0$. Furthermore, let us abandon for a moment the assumption that the state of the bath is narrowed, and take $\rho_I \sim 1$.

This case is of course exactly solvable,[59] and in the large-N limit the results are equivalent to the classical calculation,[60] in which the bath is assumed to be static, and the central spin dynamics is calculated by averaging the spin precession over a Gaussian ensemble of nuclear polarization vectors $\mathbf{B}_I$ of the form $P(\mathbf{B}_I^2) \sim \exp(-\mathbf{B}_I^2/2\sigma^2)$, where $\sigma^2 = \frac{1}{3} \sum_k I_k(I_k + 1)A_k^2$. A simple Gaussian integral gives the well-known $\exp[-(t/T_2^*)^2]$ decay of the envelope of the FID signal, with $T_2^* = \sqrt{2}/\sigma$. For large N, this is practically equivalent to the evaluation of the quantum expression

$$\langle S^+(t) \rangle = \frac{1}{2^N} e^{i\Omega t} \sum_{n_i} \exp\left(i h_{n_i}^z t \right) \langle S^+(0) \rangle. \quad (129)$$

Note that, in the above expression, every $|n_i\rangle$ state present in $\rho_I(0)$ contributes a frequency $h_{n_i}^z$, and the averaging of these frequencies leads to dephasing (inhomogeneous broadening).

It was noticed before that the standard NZ approach, when carried out to a finite order in the expansion (in powers of h_z in this case), cannot reproduce the above simple solution.[59] On the other hand, the TCL approach gives the exact result already in the second order of expansion. This feature can be traced back to the fact that in the NZ expansion, one obtains so-called *partial cumulants*[43,59] of the bath operators

(i.e. $\langle h_z^4 \rangle_{\text{pc}} = \langle h_z^4 \rangle - \langle h_z^2 \rangle^2$ appears in the fourth order), while in the TCL calculation one encounters the *ordered cumulants* (i.e., $\langle h_z^4 \rangle_{\text{oc}} = \langle h_z^4 \rangle - 3\langle h_z^2 \rangle^2$), which are clearly closely related to the usual cumulants. For the Gaussian bath, the ordered cumulants beyond second order are identically zero, and the TCL approach succeeds because it captures the crucial statistical properties of the bath already in the second order of the expansion.[61] The NZ approach, on the other hand, is incompatible with the structure of the bath correlators, and it has to be carried out to infinite order to recover the Gaussian decay of the transverse spin.

B. Uniform coupling model as a classical non-Gaussian bath

The effective-Hamiltonian-based RDT solution for dephasing in the uniform coupling model, Eq. (124), which is the same as the large-N limit of the exact solution [see the discussion leading to Eq. (128)], can also be obtained from a classical calculation.[4] We simply fix the B_I^z component of the nuclear field, perform the Gaussian average of the classical equations of motion for $S^{x,y}$, and recover the RDT results. The fast oscillation of the exact solution is clearly an effect which is being missed by the classical large-N limit. The same result is obtained when one employs the classical limit of the effective Hamiltonian, $S^z[(B_I^x)^2 + (B_I^y)^2]/2\Omega$ (as was done for the spin-echo case in Ref. 31), and performs the Gaussian average over all the precession frequencies due to the possible magnitudes of the transverse nuclear field. This shows that the RDT (at short times in the general case) and the uniform coupling calculations are essentially equivalent to classical averaging over the *square* of a Gaussian-distributed classical variable. The latter approach was successfully applied to the calculation of the Rabi oscillation decay of spin qubits.[62–65]

In the case of a bath operator coupling which is the square of a Gaussian-distributed variable, the bath correlators are such that cumulants of all orders are nonzero. However, these cumulants are simply the ring diagrams,[26,44] and the summation of all of them can be performed. In order to achieve this, it is crucial to use a theoretical approach in which the standard, i.e., ordered, cumulants appear in a natural fashion, as occurs in the effective-Hamiltonian-based RDT calculation, or in the TCL approach.[43]

As we discussed in the previous section, the standard (single-projector) NZ theory does not have a natural relation with the statistical properties of the bath, specifically with the structure of the ordered cumulants of the bath variables. Furthermore, in the standard NZ approach we project on a single tensor product state of the system and a fixed state of the environment [chosen here, as is usually done, to be $\rho_I(0)$]. The Ising coupling case clearly shows that this can a suboptimal approximation: in this case, the central spin coherence decays *only* due to the fact that the exact density matrix at finite times possesses a nontrivial structure deriving from the evolution of each of the nuclear states present in $\rho_I(0)$, i.e., in Eq. (129) we have a sum over all the $|n_i\rangle$ states, and each state contributes a different frequency. What is explicitly shown in the exact solution of the uniform coupling model is the fact that, even for the narrowed state of the bath, this is the case. The exact solution in Eq. (25) involves a sum over

the j quantum numbers: in order to obtain the correct result, one has to preserve the structure of the nuclear density matrix which is singled out by its coupling to the central spin (i.e., the nontrivial dynamics in the $j, m, m \pm 1$ subspaces). In the classical limit this averaging over the nuclear states present in the narrowed density matrix is expressed by integration over the B_I^x and B_I^y components of the nuclear field. The RDT calculation captures correctly this averaging by a proper resummation of all the diagrams relevant in the large-N limit. The NZ-CP calculation simply preserves the key structure of the total density matrix during the system's evolution, and in this way recovers the classical averaging limit.

C. Consequences for the nonuniform coupling theory

As noted in Ref. 22, the single-projector approach is expected to be valid when the system-environment coupling is weak in some sense. As shown in Refs. 9, 23, and 28, in the case of the hf-coupled spin bath this "weak coupling" condition is $\mathcal{A}/\Omega < 1$, and it apparently guarantees that the single-projector approach is valid at all times. Under this condition the short-time ($t \ll N/\mathcal{A}$) decay is very small, i.e., a quadratic initial decay, $x(t) \approx 1 - 2(t/\tau)^2$ with $t \ll \tau$. This result *does not* depend on the shape of the electron wave funtion. The decay at longer times is due to the fluctuations of the Overhauser field induced by flip-flops involving nuclei with different couplings to the central spin; the inhomogeneity of couplings is crucial at this time scale. Most of the decay for $\mathcal{A}/\Omega \ll 1$ is of the exponential form recovered by the RDT calculation. With decreasing Ω, the nonexponential features of the single-projector NZ solution become more prominent, but the form of the NFID at low fields $\Omega < \mathcal{A}$ cannot be determined in a controlled fashion,[28] at least for realistic values of nuclear spin $I > 1/2$ and for zero or small nuclear polarization.

At short times, the RDT solution remains controlled (as long as one believes in the robustness of the transformation leading to the effective Hamiltonian *on this time scale*) when $\Omega \gg \mathcal{A}/\sqrt{N}$. In this regime, the RDT solution is explicitly independent of the shape of the electron wave function,[25,26] as was the case for the short-time NZ result.[28] This agrees with the intuition that at this time scale all the internuclear flip-flops should be virtual, and all of them should be equally important. It suggests that on short time scales it should be possible to map the dynamics of the real system onto the dynamics of a model system with uniform couplings.[26,36] As we have shown here, the RDT reproduces the envelope of the exact result in this case, while the standard NZ approach fails beyond very short times, $t < \tau = 4N\Omega/\mathcal{A}^2$ (at which the envelope is well described by the quadratic decay), suggesting that the latter approach is indeed unable to describe the low-field decay, most of which occurs at short times ($t < N/\mathcal{A}$). This is consistent with the results of Refs. 9,23, and 28, in which only high fields were considered (or a large nuclear polarization was assumed), and the single-projector NZ theory was shown to be very hard to control at low fields. It should be noted, however, that the broadening of the energy bandwidth available for multiple internuclear flip-flops in higher orders in V_{ff}, discussed briefly in Ref. 28, shows that the boundary of the short-time regime can move to even shorter times as

one goes to a higher order in the expansion of the NZ memory kernel. It is nevertheless unclear what happens to this trend as the expansion is continued to higher orders. The previous discussion suggests that in order for a single-projector NZ approach to recover the uniform coupling bath limit one has to go to an infinite order in the memory kernel expansion. This makes it hard to perturbatively delineate, within the single-projector NZ approach, the time scale on which the uniform coupling model gives a good approximation to the real problem. A full-Hamiltonian approach, starting from an assumption that the box model holds on some time scale and correctly describing the decoherence in a broad range of magnetic fields, should shed more light on these issues.

The use of correlated projection operators[22,24,43] makes the second-order NZ result agree very well with both the envelope and the small oscillations of the exact result for NFID decay in the uniform coupling case. This strongly suggests that the correlated projection operator technique should be an important element of a theory of central spin decoherence encompassing all the regimes of magnetic fields and time scales.

VII. CONCLUSIONS

In this paper, we have applied the Nakajima-Zwanzig generalized master equation, originally developed for the hyperfine-coupled central spin problem in Refs. 9,23 and 28, to the exactly solvable case of uniform hyperfine couplings. We have shown that the NZ calculation of narrowed-state free-induction decay, i.e., the evolution of the electron coupled to a nuclear bath acting on it with a well-defined Overhauser field, fails very quickly in this case, and can only account for the initial decoherence dynamics. We have traced the origin of this failure to the fact that, in this NZ approach, a single operator was used to project the total density matrix onto the tensor product of the central spin and bath density matrices. While this approach works well at high magnetic fields, at which the coherence decays at long times, and the inhomogeneity of the electron's wave function (i.e., the inhomogeneity of the hf couplings) is crucial for the coherence decay,[23,28] it fails at short times and low fields, at which the shape of the wave function should be irrelevant, and the uniform coupling model is expected to be applicable. In the latter situation, one has to modify the NZ approach by introducing a family of correlated projection operators,[22,24] with which one can capture the essential features of the exact dynamics: the electron loses its coherence by a rather simple dephasing process, in which the electron spin states acquire a different phase when interacting with nuclear states from different subspaces, and the coherence is lost due to averaging over the initial nuclear states. With this modification, the NZ GME reproduces very well the exact solution for the uniform coupling model.

The exact result for NFID in the uniform coupling model is also reproduced by the effective-Hamiltonian-based solution from Refs. 25 and 26 on a time scale long enough to capture the full coherence decay. This is another example of the effective-Hamiltonian-based theory[25,26] reproducing the semiclassical limit (i.e., the quantum calculation being equivalent to an average over classical nuclear fields) of the central spin dephasing problem.[31]

According to the effective-Hamiltonian-based theory, NFID should be described by Eq. (124) up to a time scale of $\sim$10 μs in GaAs dots (with $N \approx 10^6$), and this decay will be significant for magnetic fields smaller than 1 T. The NFID measurements in this parameter range are within reach of the fast measurement techniques developed for gated GaAs dots.[39] Upon increasing the magnetic field, the decoherence times calculated from the purely hf central spin Hamiltonian quickly become comparable to the predicted decay times due to dipolar-induced spectral diffusion,[12,52] which were obtained with the cluster methods succesfully describing the high-field decay of the spin-echo signal in GaAs.[48] This probably makes the long-time regime (the exponential decay) very hard to observe in large GaAs dots. On the other hand, in InGaAs dots, especially the smallest ones ($N \approx 10^4$), the short-time regime extends to at most $\sim$100 ns, and the low-field requirement might be incompatible with the spin splitting needed for the optical manipulation of the qubit. These dots seem to be more suited for experimentally investigating the high-field and long-time regime of exponential decay since the predicted[52] decoherence times due to the nuclear dipolar interactions are on the order of 5–10 μs (which is a lower bound since quadrupolar interactions were not included in that theory), giving a window of time scales in which the decay due to the hf interaction only could be observed. The exponential decay was indeed seen in such dots,[37] but more research is needed to ascertain its magnetic field dependence. If the nuclear-state narrowing could be done in InGaAs dots at lower magnetic fields (e.g., around 1 T and possibly below), the crossover between the short and long time scales should be seen, making it possible to check the time scale at which the uniform coupling model predictions hold and to verify the predictions of Ref. 28 in the $\Omega \approx \mathcal{A}$ regime, in which the single-projector NZ results differ significantly from the effective-Hamiltonian results.

The results of this paper make a strong statement regarding the structure of a theory which could describe the electron spin decoherence without the use of an effective Hamiltonian in a broad range of magnetic fields. In order to properly describe the short-time ($t \ll N/\mathcal{A}$) regime, in which the coherence is expected to decay at low magnetic fields, one should employ the correlated projection operator approach in the derivation of a generalized master equation. This was done employing both the NZ and the time-convolutionless methods in the uniform[22] and nonuniform[24] coupling cases (in the latter case using only the projectors of spaces of fixed m, not the jm spaces used here), albeit only for a thermal nuclear bath. In this work we have shown that this feature of the theory is crucial also in the case of NFID and uniform couplings. The case of low-field NFID in a realistic inhomogenously coupled system remains to be further investigated. While we have focused here on the NZ approach, which was the subject of intense research[9,23,28] in the context of NFID, it might turn out that the TCL approach (untested yet for NFID) will be both easier to implement and more natural. The latter statement is supported by the fact that the structure of TCL is closer to the cumulant expansion structure which underpins the effective-Hamiltonian solution from Refs. 25 and 26. These theories not only practically agree

with the NZ approach at high fields in the nonuniform coupling case but also capture correctly the exact solution in the uniform coupling case, strongly suggesting that they correctly describe the low-field and short-time decay of NFID, just as they correctly described the spin-echo signal.[31,48] However, the nature of the crossover between the high-field/long-time, and low-field/short-time decay behaviors remains to be elucidated using a theory capable of treating both regimes on equal footing.

APPENDIX A: THE FULL EXPRESSION FOR THE FOURTH-ORDER MEMORY KERNEL

In this section, we will work out the explicit form for the Laplace transform of the fourth-order memory kernel. We will not make any assumptions about the distribution of hyperfine couplings or about the magnitude of Ω relative to other scales in the problem. The only assumption is that the initial nuclear density matrix has the form shown in Eq. (12). Starting from Eq. (70), we replace each occurrence of $G(s)$ with $\int_0^\infty dt\, e^{-st} G(t)$ to obtain

$$\Sigma^{(4)}(s) = i \int_0^\infty \prod_{i=1}^4 dt_i e^{-s \sum_i t_i} \mathrm{Tr}\{S^+[s - iL_0 Q G(t_1)] L_V G(t_2) L_V Q G(t_3) L_V G(t_4) L_V S^- \rho_I(0)\}. \tag{A1}$$

This step allows us to work with $G(t)$ as opposed to its Laplace transform, making it easier to find explicit expressions. We will evaluate the string of operators appearing inside the trace in two stages. First consider

$$T \equiv G(t_3) L_V G(t_4) L_V S^- \rho_I(0). \tag{A2}$$

We can evaluate this using Eqs. (55) and (56), finding

$$T = \begin{pmatrix} 0 & T_{\uparrow\downarrow} \\ T_{\downarrow\uparrow} & 0 \end{pmatrix}, \tag{A3}$$

with

$$T_{\uparrow\downarrow} = \sum_{k\ell} \tilde{a}_{k\ell} I_\ell^- \rho_I(0) I_k^-,$$
$$T_{\downarrow\uparrow} = \sum_{k\ell} [\tilde{b}_{k\ell} I_\ell^+ I_k^- \rho_I(0) + \tilde{c}_{k\ell} \rho_I(0) I_k^- I_\ell^+], \tag{A4}$$

where

$$\tilde{a}_{k\ell} = -\tfrac{1}{4} A_k A_\ell e^{-i[\Omega_n - \omega_k - \omega_\ell + (1/2)(A_k - A_\ell)]t_3} [e^{i(\omega_k - A_k/2)t_4} + e^{i(\omega_\ell + A_\ell/2)t_4}],$$
$$\tilde{b}_{k\ell} = \tfrac{1}{4} A_k A_\ell e^{i[\Omega_n + \omega_k - \omega_\ell - (1/2)(A_k - A_\ell)]t_3} e^{i(\omega_k + A_k/2)t_4}, \tag{A5}$$
$$\tilde{c}_{k\ell} = \tfrac{1}{4} A_k A_\ell e^{i[\Omega_n + \omega_k - \omega_\ell + (1/2)(A_k - A_\ell)]t_3} e^{i(\omega_k - A_k/2)t_4}.$$

For the second stage of the evaluation, we define

$$R \equiv L_V G(t_2) L_V Q T. \tag{A6}$$

Given the structure of T, Eq. (A3), it is not difficult to show that R has a similar form:

$$R = \begin{pmatrix} 0 & R_{\uparrow\downarrow} \\ R_{\downarrow\uparrow} & 0 \end{pmatrix}. \tag{A7}$$

In terms of R, we may write the trace in Eq. (A1) as

$$\mathrm{Tr}\{S^+[s - iL_0 Q G(t_1)] R\} = \mathrm{Tr}\{\Delta_1 R_{\downarrow\uparrow}\}, \tag{A8}$$

with

$$\Delta_1 \equiv s + i(h^z - h_n^z) e^{i(\Omega + h^z)t_1}. \tag{A9}$$

Therefore, it is only necessary to compute one of the components of R, and this can be expressed in terms of T according to

$$R_{\downarrow\uparrow} = \tfrac{1}{4} h^+ U_+(t_2)\{h^- T_{\downarrow\uparrow} - h^- \rho_I(0)\mathrm{Tr}[T_{\downarrow\uparrow}] - T_{\uparrow\downarrow} h^+\} U_+^\dagger(t_2) - \tfrac{1}{4} U_-(t_2)\{h^+ T_{\uparrow\downarrow} - T_{\downarrow\uparrow} h^- + \rho_I(0)\mathrm{Tr}[T_{\downarrow\uparrow}] h^-\} U_-^\dagger(t_2) h^+, \tag{A10}$$

where $U_\pm(t)$ were defined in Eq. (54). The explicit form of the trace, Eq. (A8), is rather messy, so we first break it up into four parts in an effort to improve readability:

$$\text{Tr}\{\Delta_1 R_{\downarrow\uparrow}\} = \sum_{i=1}^{4} X_i, \tag{A11}$$

$$
\begin{aligned}
X_1 &= -\tfrac{1}{4}\text{Tr}\{\Delta_1 h^+ U_+(t_2) T_{\uparrow\downarrow} h^+ U_+^\dagger(t_2)\} - \tfrac{1}{4}\text{Tr}\{\Delta_1 U_-(t_2) h^+ T_{\uparrow\downarrow} U_-^\dagger(t_2) h^+\}, \\
X_2 &= -\tfrac{1}{4}\text{Tr}[T_{\downarrow\uparrow}]\text{Tr}\{\Delta_1 h^+ U_+(t_2) h^- \rho_I(0) U_+^\dagger(t_2)\} - \tfrac{1}{4}\text{Tr}[T_{\downarrow\uparrow}]\text{Tr}\{\Delta_1 U_-(t_2)\rho_I(0) h^- U_-^\dagger(t_2) h^+\}, \\
X_3 &= \tfrac{1}{4}\text{Tr}\{\Delta_1 h^+ U_+(t_2) h^- T_{\downarrow\uparrow} U_+^\dagger(t_2)\}, \\
X_4 &= \tfrac{1}{4}\text{Tr}\{\Delta_1 U_-(t_2) T_{\downarrow\uparrow} h^- U_-^\dagger(t_2) h^+\}.
\end{aligned}
\tag{A12}
$$

These evaluate to

$$X_1 = -\frac{1}{4}\sum_{k\ell pq} \tilde{a}_{k\ell} A_p A_q [e^{i(\omega_p + A_p/2)t_2} + e^{i(\omega_q - A_q/2)t_2}][s + i(A_p - A_\ell)e^{i(\Omega_n + A_p - A_\ell)t_1}]\text{Tr}\{I_p^+ I_\ell^- \rho_I(0) I_k^- I_q^+\}, \tag{A13}$$

$$X_2 = -\frac{s}{16}e^{i\Omega_n t_3}\sum_{k\ell} A_k^2 A_\ell^2 e^{i\omega_\ell t_2} e^{i\omega_k t_4}[c_\ell^- e^{i(A_\ell/2)t_2} + c_\ell^+ e^{-i(A_\ell/2)t_2}][c_k^- e^{i(A_k/2)t_4} + c_k^+ e^{-i(A_k/2)t_4}], \tag{A14}$$

$$X_3 = \frac{1}{4}\sum_{k\ell pq} A_p A_q e^{i(\omega_p + A_p/2)t_2}\{s\tilde{b}_{k\ell}\text{Tr}\{I_\ell^+ I_k^- \rho_I(0) I_p^+ I_q^-\} + \tilde{c}_{k\ell}[s + i(A_p - A_q)e^{i(\Omega_n + A_p - A_q)t_1}]\text{Tr}\{I_p^+ I_q^- \rho_I(0) I_k^- I_\ell^+\}\}, \tag{A15}$$

$$X_4 = \frac{1}{4}\sum_{k\ell pq} A_p A_q e^{i(\omega_p - A_p/2)t_2}\{s\tilde{c}_{k\ell}\text{Tr}\{I_q^- I_p^+ \rho_I(0) I_k^- I_\ell^+\} + \tilde{b}_{k\ell}[s + i(A_\ell - A_k)e^{i(\Omega_n + A_\ell - A_k)t_1}]\text{Tr}\{I_\ell^+ I_k^- \rho_I(0) I_q^- I_p^+\}\}. \tag{A16}$$

Performing the fourfold Laplace transform in Eq. (A1) on each of the X_i and denoting the results by Y_i, we find

$$
\begin{aligned}
Y_1 &= \frac{1}{16}\sum_{k\ell pq} A_k A_\ell A_p A_q \frac{\text{Tr}\{I_p^+ I_\ell^- \rho_I(0) I_k^- I_q^+\}}{s + i\left[\Omega_n - \omega_k - \omega_\ell + \frac{1}{2}(A_k - A_\ell)\right]}\left[1 + i\frac{A_p - A_\ell}{s - i(\Omega_n + A_p - A_\ell)}\right] \\
&\quad \times \left[\frac{1}{s - i\left(\omega_p + \frac{A_p}{2}\right)} + \frac{1}{s - i\left(\omega_q - \frac{A_q}{2}\right)}\right]\left[\frac{1}{s - i\left(\omega_\ell + \frac{A_\ell}{2}\right)} + \frac{1}{s - i\left(\omega_k - \frac{A_k}{2}\right)}\right],
\end{aligned}
\tag{A17}
$$

$$Y_2 = -\frac{1}{16}\sum_{k\ell} A_k^2 A_\ell^2 \frac{1}{s - i\Omega_n}\left[\frac{c_k^-}{s - i\left(\omega_k + \frac{A_k}{2}\right)} + \frac{c_k^+}{s - i\left(\omega_k - \frac{A_k}{2}\right)}\right]\left[\frac{c_\ell^-}{s - i\left(\omega_\ell + \frac{A_\ell}{2}\right)} + \frac{c_\ell^+}{s - i\left(\omega_\ell - \frac{A_\ell}{2}\right)}\right], \tag{A18}$$

$$
\begin{aligned}
Y_3 &= \frac{1}{16}\sum_{k\ell pq} A_k A_\ell A_p A_q \frac{1}{s - i\left(\omega_p + \frac{A_p}{2}\right)}\left\{\frac{1}{s - i\left(\omega_k + \frac{A_k}{2}\right)}\frac{\text{Tr}\{I_\ell^+ I_k^- \rho_I(0) I_p^+ I_q^-\}}{s - i\left[\Omega_n + \omega_k - \omega_\ell - \frac{1}{2}(A_k - A_\ell)\right]}\right. \\
&\quad \left. + \frac{1}{s - i\left(\omega_k - \frac{A_k}{2}\right)}\frac{\text{Tr}\{I_p^+ I_q^- \rho_I(0) I_k^- I_\ell^+\}}{s - i\left[\Omega_n + \omega_k - \omega_\ell + \frac{1}{2}(A_k - A_\ell)\right]}\left[1 + i\frac{A_p - A_q}{s - i(\Omega_n + A_p - A_q)}\right]\right\},
\end{aligned}
\tag{A19}
$$

$$
\begin{aligned}
Y_4 &= \frac{1}{16}\sum_{k\ell pq} A_k A_\ell A_p A_q \frac{1}{s - i(\omega_p - \frac{A_p}{2})}\left\{\frac{1}{s - i\left(\omega_k - \frac{A_k}{2}\right)}\frac{\text{Tr}\{I_q^- I_p^+ \rho_I(0) I_k^- I_\ell^+\}}{s - i\left[\Omega_n + \omega_k - \omega_\ell + \frac{1}{2}(A_k - A_\ell)\right]}\right. \\
&\quad \left. + \frac{1}{s - i\left(\omega_k + \frac{A_k}{2}\right)}\frac{\text{Tr}\{I_\ell^+ I_k^- \rho_I(0) I_q^- I_p^+\}}{s - i\left[\Omega_n + \omega_k - \omega_\ell - \frac{1}{2}(A_k - A_\ell)\right]}\left[1 + i\frac{A_\ell - A_k}{s - i(\Omega_n + A_\ell - A_k)}\right]\right\}.
\end{aligned}
\tag{A20}
$$

The Laplace transform of the fourth-order memory kernel is given by

$$\Sigma^{(4)}(s) = i\sum_{i=1}^{4} Y_i(s). \tag{A21}$$

In the high-frequency limit, we have in the rotating frame defined by Ω_n $[\bar{Y}_i = Y_i(s + i\Omega_n)]$

$$\bar{Y}_1 \approx 0, \tag{A22}$$

$$\bar{Y}_2 \approx \frac{1}{16\Omega_n^2} \sum_{k\ell} A_k^2 A_\ell^2 [c_k^- + c_k^+][c_\ell^- + c_\ell^+] \frac{1}{s}, \tag{A23}$$

$$\bar{Y}_3 \approx -\frac{1}{16\Omega_n^2} \sum_{k\ell pq} A_k A_\ell A_p A_q \left[\frac{\mathrm{Tr}\{I_\ell^+ I_k^- \rho_I(0) I_p^+ I_q^-\}}{s - i\left[\omega_k - \omega_\ell - \frac{1}{2}(A_k - A_\ell)\right]} + \frac{s}{s - i(A_p - A_q)} \frac{\mathrm{Tr}\{I_p^+ I_q^- \rho_I(0) I_k^- I_\ell^+\}}{s - i\left[\omega_k - \omega_\ell + \frac{1}{2}(A_k - A_\ell)\right]} \right], \quad \text{(A24)}$$

$$\bar{Y}_4 \approx -\frac{1}{16\Omega_n^2} \sum_{k\ell pq} A_k A_\ell A_p A_q \left[\frac{\mathrm{Tr}\{I_q^- I_p^+ \rho_I(0) I_k^- I_\ell^+\}}{s - i\left[\omega_k - \omega_\ell + \frac{1}{2}(A_k - A_\ell)\right]} + \frac{s}{s - i(A_\ell - A_k)} \frac{\mathrm{Tr}\{I_\ell^+ I_k^- \rho_I(0) I_q^- I_p^+\}}{s - i\left[\omega_k - \omega_\ell - \frac{1}{2}(A_k - A_\ell)\right]} \right], \quad \text{(A25)}$$

and

$$\Sigma^{(4)}(s + i\Omega_n) = \bar{\Sigma}(s) = i \sum_{i=1}^4 \bar{Y}_i(s). \tag{A26}$$

APPENDIX B: NUCLEAR BATH CORRELATORS

In this Appendix, we evaluate the nuclear bath correlators which arise in the expression for the fourth-order memory kernel. For example, in the expression given for Y_3 in Appendix A, there appears the correlator

$$\mathrm{Tr}\{I_p^+ I_q^- \rho_I(0) I_k^- I_\ell^+\}. \tag{B1}$$

Since $\rho_I(0)$ is assumed to be diagonal in the $|n_i\rangle$ basis, this correlator is only nonzero when each pair of raising and lowering operators act on the same nucleus, and we obtain

$$\mathrm{Tr}\{I_p^+ I_q^- \rho_I(0) I_k^- I_\ell^+\}$$
$$= [\delta_{k\ell}\delta_{pq} + \delta_{kp}\delta_{\ell q}(1 - \delta_{kq})] \sum_i \rho_{ii} c_k^{(i)+} c_q^{(i)-}, \tag{B2}$$

where we have defined

$$c_k^{(i)\pm} \equiv \langle n_i | I_k^\mp I_k^\pm | n_i \rangle = I_k(I_k + 1) - (m_k^i)^2 \mp m_k^i. \tag{B3}$$

Recall that I_k is the total spin of the kth nucleus and that m_k^i is the eigenvalue of I_k^z associated with the state $|n_i\rangle$. (The total spin of the kth nucleus depends on k since we have incorporated information about different species into the nuclear site index k.) These quantities are related to the correlators $c_k^\pm$ according to

$$c_k^\pm \equiv \mathrm{Tr}\{I_k^\mp I_k^\pm \rho_I(0)\} = \sum_i \rho_{ii} c_k^{(i)\pm}. \tag{B4}$$

We may express the other four correlators appearing in the Y_i in terms of the $c_k^{(i)\pm}$:

$$\mathrm{Tr}\{I_p^+ I_\ell^- \rho_I(0) I_k^- I_q^+\}$$
$$= [\delta_{kq}\delta_{\ell p} + \delta_{kp}\delta_{\ell q}(1 - \delta_{k\ell})] \sum_i \rho_{ii} c_k^{(i)+} c_\ell^{(i)-},$$

$$\mathrm{Tr}\{I_\ell^+ I_k^- \rho_I(0) I_q^- I_p^+\}$$
$$= [\delta_{k\ell}\delta_{pq} + \delta_{kp}\delta_{\ell q}(1 - \delta_{kq})] \sum_i \rho_{ii} c_k^{(i)-} c_q^{(i)+},$$

$$\mathrm{Tr}\{I_\ell^+ I_k^- \rho_I(0) I_p^+ I_q^-\} \tag{B5}$$
$$= \sum_i \rho_{ii} \left[\delta_{k\ell}\delta_{pq} c_k^{(i)-} c_q^{(i)-} + \delta_{kp}\delta_{\ell q}(1 - \delta_{kq}) c_k^{(i)-} c_q^{(i)+}\right],$$

$$\mathrm{Tr}\{I_q^- I_p^+ \rho_I(0) I_k^- I_\ell^+\}$$
$$= \sum_i \rho_{ii} \left[\delta_{k\ell}\delta_{pq} c_k^{(i)+} c_q^{(i)+} + \delta_{kp}\delta_{\ell q}(1 - \delta_{kq}) c_k^{(i)+} c_q^{(i)-}\right].$$

As an aside, we note that in the case of a uniformly polarized homonuclear bath, the two-operator correlators become independent of k:

$$c^\pm = c_k^\pm = \sum_i \rho_{ii} c_k^{(i)\pm}. \tag{B6}$$

For the case of spin-1/2 nuclei, these are particularly simple,

$$c^\pm = \frac{1}{2} \mp \sum_i \rho_{ii} m_k^i = \frac{1}{2} \mp \frac{m}{N}, \tag{B7}$$

where m is the net polarization of all the nuclei defined by

$$m \equiv \sum_i \rho_{ii} \sum_k m_k^i. \tag{B8}$$

For a uniformly polarized nuclear bath, m is closely related to the quantity h_n^z defined in Eq. (34):

$$m = \frac{N h_n^z}{\mathcal{A}}. \tag{B9}$$

Next, we will prove a relation which is useful for simplifying the correlators in Eq. (B5). In particular, we want to show that in the case of a uniformly polarized nuclear spin bath, we have

$$\sum_i \rho_{ii} c_k^{(i)+} c_\ell^{(i)-} = \left(\sum_i \rho_{ii} c_k^{(i)+}\right)\left(\sum_i \rho_{ii} c_\ell^{(i)-}\right) = c^+ c^-. \tag{B10}$$

In the final expression, we have used the fact that the condition of uniform polarization implies that the result is independent of the nuclear site indices k and ℓ. We have also implicitly

assumed a homonuclear bath since information about different nuclear species is incorporated into the site index. This last assumption can easily be relaxed by retaining this information in the form of an additional index; however, in the situations in this paper where Eq. (B10) is employed, the homonuclear assumption is made anyway for the sake of simplicity. Also note that we are not assuming spin-1/2 nuclei in Eq. (B10). Replacing the $c_k^{(i)\pm}$ with explicit expressions from Eq. (B3) and canceling several terms, we obtain

$$\sum_i \rho_{ii} c_k^{(i)+} c_\ell^{(i)-} - \left(\sum_i \rho_{ii} c_k^{(i)+}\right)\left(\sum_i \rho_{ii} c_\ell^{(i)-}\right)$$

$$= \sum_i \rho_{ii} (m_k^i)^2 (m_\ell^i)^2 - \left(\sum_i \rho_{ii} (m_k^i)^2\right)\left(\sum_i \rho_{ii} (m_\ell^i)^2\right)$$

$$- \sum_i \rho_{ii} (m_k^i)^2 m_\ell^i + \left(\sum_i \rho_{ii} (m_k^i)^2\right)\left(\sum_i \rho_{ii} m_\ell^i\right)$$

$$+ \sum_i \rho_{ii} m_k^i (m_\ell^i)^2 - \left(\sum_i \rho_{ii} m_k^i\right)\left(\sum_i \rho_{ii} (m_\ell^i)^2\right)$$

$$- \sum_i \rho_{ii} m_k^i m_\ell^i + \left(\sum_i \rho_{ii} m_k^i\right)\left(\sum_i \rho_{ii} m_\ell^i\right). \quad \text{(B11)}$$

Each term in Eq. (B11) is independent of k and ℓ in the uniformly polarized case, so that the second and third lines on the right-hand side of the equation vanish identically. Consider the term $\sum_i \rho_{ii} m_k^i m_\ell^i$ in the last line. We can multiply this by $A_k A_\ell$ and sum over k and ℓ. Since the $|n_i\rangle$ states all have the same h^z eigenvalue, we know that

$$\sum_{k\ell} A_k A_\ell m_k^i m_\ell^i = (h_n^z)^2 \quad \text{(B12)}$$

is independent of i. On the other hand, $\sum_i \rho_{ii} m_k^i m_\ell^i$ is independent of k and ℓ, so that multiplying by $A_k A_\ell$ and summing over k and ℓ simply amounts to multiplying this expression by $(\sum_k A_k)^2 = \mathcal{A}^2$. These two observations together imply that

$$\sum_i \rho_{ii} m_k^i m_\ell^i = \left(\frac{h_n^z}{\mathcal{A}}\right)^2. \quad \text{(B13)}$$

From Eq. (B9) we have

$$\sum_i \rho_{ii} m_k^i = \frac{m}{N} = \frac{h_n^z}{\mathcal{A}}, \quad \text{(B14)}$$

showing that the last two terms on the right-hand side of Eq. (B11) cancel each other.

To finish the proof of Eq. (B10), it remains to show that the first line on the right-hand side of Eq. (B11) vanishes. This follows straightforwardly from a simple generalization of the previous argument. We begin with the following expression:

$$\sum_i \rho_{ii} m_k^i m_\ell^i m_p^i m_q^i - \left(\sum_i \rho_{ii} m_k^i m_p^i\right)\left(\sum_i \rho_{ii} m_\ell^i m_q^i\right). \quad \text{(B15)}$$

We can evaluate explicitly each of the two terms by multiplying by $A_k A_\ell A_p A_q / \mathcal{A}^4$ and summing over k,ℓ,p,q. Since each term is independent of k,ℓ,p,q under the assumption of uniform polarization, this procedure should leave the terms unchanged. We find that the two terms evaluate to the same expression and thus cancel:

$$\sum_i \rho_{ii} m_k^i m_\ell^i m_p^i m_q^i - \left(\sum_i \rho_{ii} m_k^i m_p^i\right)\left(\sum_i \rho_{ii} m_\ell^i m_q^i\right)$$

$$= \left(\frac{h_n^z}{\mathcal{A}}\right)^4 - \left(\frac{h_n^z}{\mathcal{A}}\right)^4 = 0. \quad \text{(B16)}$$

The first line on the right-hand side of Eq. (B11) is just a special case of Eq. (B15) where $p = k$ and $q = \ell$, so we have also shown that this line vanishes, completing the proof of Eq. (B10). Repeated application of these arguments can be used to show more generally that

$$\sum_i \rho_{ii} c_k^{(i)\pm} c_\ell^{(i)\pm} = c^\pm c^\pm, \quad \text{(B17)}$$

where here the two sets of $\pm$ signs are independent of each other.

The identity in Eq. (B17) is used extensively in the context of the high-frequency limit considered in Sec. IV E. We can also use it to simplify the four-operator correlators in Eq. (B5). In the uniform coupling model, the indices of these correlators are summed over, so we have

$$\sum_{k\ell pq} \text{Tr}\{I_p^+ I_\ell^- \rho_I(0) I_k^- I_q^+\} = \sum_{k\ell pq} \text{Tr}\{I_p^+ I_q^- \rho_I(0) I_k^- I_\ell^+\}$$

$$= \sum_{k\ell pq} \text{Tr}\{I_\ell^+ I_k^- \rho_I(0) I_q^- I_p^+\} = 2N^2 c^+ c^-,$$

$$\times \sum_{k\ell pq} \text{Tr}\{I_\ell^+ I_k^- \rho_I(0) I_p^+ I_q^-\} = N^2 c^-,$$

$$\times \sum_{k\ell pq} \text{Tr}\{I_q^- I_p^+ \rho_I(0) I_k^- I_\ell^+\} = N^2 c^+. \quad \text{(B18)}$$

These relations were used to obtain Eqs. (75) and (76).

*barnes@umd.edu

†lcyw@ifpan.edu.pl

[1] R. Hanson, L. P. Kouwenhoven, J. R. Petta, S. Tarucha, and L. M. K. Vandersypen, Rev. Mod. Phys. **79**, 1217 (2007).

[2] R.-B. Liu, W. Yao, and L. J. Sham, Adv. Phys. **59**, 703 (2010).

[3] W. A. Coish and J. Baugh, Phys. Status Solidi B **246**, 2203 (2009).

[4] Ł. Cywiński, Acta Phys. Pol. A **119**, 576 (2011).

[5] A. V. Khaetskii, D. Loss, and L. Glazman, Phys. Rev. Lett. **88**, 186802 (2002).

[6] J. Schliemann, A. V. Khaetskii, and D. Loss, Phys. Rev. B **66**, 245303 (2002).

[7] A. Khaetskii, D. Loss, and L. Glazman, Phys. Rev. B **67**, 195329 (2003).

[8] V. V. Dobrovitski and H. A. De Raedt, Phys. Rev. E **67**, 056702 (2003).

[9] W. A. Coish and D. Loss, Phys. Rev. B **70**, 195340 (2004).

[10] S. I. Erlingsson and Y. V. Nazarov, Phys. Rev. B **70**, 205327 (2004).

[11] N. Shenvi, R. de Sousa, and K. B. Whaley, Phys. Rev. B **71**, 224411 (2005).

[12] W. Yao, R.-B. Liu, and L. J. Sham, Phys. Rev. B **74**, 195301 (2006).

[13] W. Zhang, V. V. Dobrovitski, K. A. Al-Hassanieh, E. Dagotto, and B. N. Harmon, Phys. Rev. B **74**, 205313 (2006).

[14] K. A. Al-Hassanieh, V. V. Dobrovitski, E. Dagotto, and B. N. Harmon, Phys. Rev. Lett. **97**, 037204 (2006).

[15] C. Deng and X. Hu, Phys. Rev. B **73**, 241303(R) (2006).

[16] R.-B. Liu, W. Yao, and L. J. Sham, New J. Phys. **9**, 226 (2007).

[17] S. K. Saikin, W. Yao, and L. J. Sham, Phys. Rev. B **75**, 125314 (2007).

[18] G. Chen, D. L. Bergman, and L. Balents, Phys. Rev. B **76**, 045312 (2007).

[19] M. Bortz and J. Stolze, Phys. Rev. B **76**, 014304 (2007).

[20] M. Bortz and J. Stolze, J. Stat. Mech. **2007**, P06018.

[21] C. Deng and X. Hu, Phys. Rev. B **78**, 245301 (2008).

[22] J. Fischer and H.-P. Breuer, Phys. Rev. A **76**, 052119 (2007).

[23] W. A. Coish, J. Fischer, and D. Loss, Phys. Rev. B **77**, 125329 (2008).

[24] E. Ferraro, H.-P. Breuer, A. Napoli, M. A. Jivulescu, and A. Messina, Phys. Rev. B **78**, 064309 (2008).

[25] Ł. Cywiński, W. M. Witzel, and S. Das Sarma, Phys. Rev. Lett. **102**, 057601 (2009).

[26] Ł. Cywiński, W. M. Witzel, and S. Das Sarma, Phys. Rev. B **79**, 245314 (2009).

[27] Ł. Cywiński, V. V. Dobrovitski, and S. Das Sarma, Phys. Rev. B **82**, 035315 (2010).

[28] W. A. Coish, J. Fischer, and D. Loss, Phys. Rev. B **81**, 165315 (2010).

[29] J. Fischer and D. Loss, Phys. Rev. Lett. **105**, 266603 (2010).

[30] M. Bortz, S. Eggert, C. Schneider, R. Stübner, and J. Stolze, Phys. Rev. B **82**, 161308 (2010).

[31] I. Neder, M. S. Rudner, H. Bluhm, S. Foletti, B. I. Halperin, and A. Yacoby, Phys. Rev. B **84**, 035441 (2011).

[32] M. Gaudin, J. Phys. (France) **37**, 1087 (1976).

[33] A. Faribault, O. El Araby, C. Sträter, and V. Gritsev, Phys. Rev. B **83**, 235124 (2011).

[34] E. A. Yuzbashyan, B. L. Altshuler, V. B. Kuznetsov, and V. Z. Enolskii, J. Phys. A **38**, 7831 (2005).

[35] W. Zhang, N. Konstantinidis, K. A. Al-Hassanieh, and V. V. Dobrovitski, J. Phys.: Condens. Matter **19**, 083202 (2007).

[36] E. Ferraro, H.-P. Breuer, A. Napoli, and A. Messina, Phys. Scr., T **140**, 014021 (2010).

[37] A. Greilich, D. R. Yakovlev, A. Shabaev, A. L. Efros, I. A. Yugova, R. Oulton, V. Stavarache, D. Reuter, A. Wieck, and M. Bayer, Science **313**, 341 (2006).

[38] C. Latta, A. Högele, Y. Zhao, A. N. Vamivakas, P. Maletinsky, M. Kroner, J. Dreiser, I. Carusotto, A. Badolato, D. Schuh et al., Nat. Phys. **5**, 758 (2009).

[39] C. Barthel, D. J. Reilly, C. M. Marcus, M. P. Hanson, and A. C. Gossard, Phys. Rev. Lett. **103**, 160503 (2009).

[40] I. T. Vink, K. C. Nowack, F. Koppens, J. Danon, Y. V. Nazarov, and L. M. K. Vandersypen, Nat. Phys. **5**, 764 (2009).

[41] S. Foletti, H. Bluhm, D. Mahalu, V. Umansky, and A. Yacoby, Nat. Phys. **5**, 903 (2009).

[42] E. Fick and G. Sauermann, The Quantum Statistics of Dynamics Processes (Springer-Verlag, Berlin, 1990).

[43] H. Breuer and F. Petruccione, The Theory of Open Quantum Systems (Oxford University Press, Oxford, 2007).

[44] Y. Makhlin and A. Shnirman, Phys. Rev. Lett. **92**, 178301 (2004).

[45] A. Grishin, I. V. Yurkevich, and I. V. Lerner, Phys. Rev. B **72**, 060509(R) (2005).

[46] R. M. Lutchyn, Ł. Cywiński, C. P. Nave, and S. Das Sarma, Phys. Rev. B **78**, 024508 (2008).

[47] W. Yang and R. B. Liu, Phys. Rev. B **77**, 085302 (2008).

[48] H. Bluhm, S. Foletti, I. Neder, M. Rudner, D. Mahalu, V. Umansky, and A. Yacoby, Nat. Phys. **7**, 109 (2011).

[49] R. de Sousa and S. Das Sarma, Phys. Rev. B **68**, 115322 (2003).

[50] W. M. Witzel, R. de Sousa, and S. Das Sarma, Phys. Rev. B **72**, 161306(R) (2005).

[51] W. M. Witzel and S. Das Sarma, Phys. Rev. B **74**, 035322 (2006).

[52] W. M. Witzel and S. Das Sarma, Phys. Rev. B **77**, 165319 (2008).

[53] W. M. Witzel, M. S. Carroll, A. Morello, Ł. Cywiński, and S. Das Sarma, Phys. Rev. Lett. **105**, 187602 (2010).

[54] E. Abe, A. M. Tyryshkin, S. Tojo, J. J. L. Morton, W. M. Witzel, A. Fujimoto, J. W. Ager, E. E. Haller, J. Isoya, S. A. Lyon et al., Phys. Rev. B **82**, 121201 (2010).

[55] R. E. George, W. Witzel, H. Riemann, N. V. Abrosimov, N. Nötzel, M. L. W. Thewalt, and J. J. L. Morton, Phys. Rev. Lett. **105**, 067601 (2010).

[56] C. Latta, A. Srivastava, and A. Imamoglu, e-print arXiv:1104.1111, Phys. Rev. Lett. (to be published).

[57] W. A. Coish, D. Loss, E. A. Yuzbashyan, and B. L. Altshuler, J. Appl. Phys. **101**, 081715 (2007).

[58] A. Melikidze, V. V. Dobrovitski, H. A. De Raedt, M. I. Katsnelson, and B. N. Harmon, Phys. Rev. B **70**, 014435 (2004).

[59] H. Krovi, O. Oreshkov, M. Ryazanov, and D. A. Lidar, Phys. Rev. A **76**, 052117 (2007).

[60] I. A. Merkulov, A. L. Efros, and M. Rosen, Phys. Rev. B **65**, 205309 (2002).

[61] R. Doll, D. Zueco, M. Wubs, S. Kohler, and P. Hanggi, Chem. Phys. **347**, 243 (2008).

[62] V. V. Dobrovitski, H. A. De Raedt, M. I. Katsnelson, and B. N. Harmon, e-print arXiv:quant-ph/0112053.

[63] J. M. Taylor and M. D. Lukin, Quantum Inf. Process. **5**, 503 (2006).

[64] F. H. L. Koppens, D. Klauser, W. A. Coish, K. C. Nowack, L. P. Kouwenhoven, D. Loss, and L. M. K. Vandersypen, Phys. Rev. Lett. **99**, 106803 (2007).

[65] R. Hanson, V. V. Dobrovitski, A. E. Feiguin, O. Gywat, and D. D. Awschalom, Science **320**, 352 (2008).